UPGRADING OF PYROLYSIS BIO-OIL BY CATALYTIC DEOXYGENATION USING CoMo AND NiMo BASED CATALYSTS

MS. SIYADA IANGMEE
ID: 54910429

A THESIS SUBMITTED AS A PART OF THE REQUIREMENTS
FOR THE DEGREE OF MASTER OF ENGINEERING
IN ENERGY TECHNOLOGY AND MANAGEMENT

THE JOINT GRADUATE SCHOOL OF ENERGY AND ENVIRONMENT
AT KING MONGKUT'S UNIVERSITY OF TECHNOLOGY THONBURI

2ND SEMESTER 2013

Upgrading of Pyrolysis Bio-Oil by Catalytic Deoxygenation
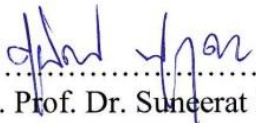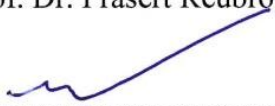Using CoMo and NiMo based Catalysts

Ms. Siyada Iangmee
ID: 54910029

A Thesis Submitted as a Part of the Requirements
for the Degree of Master of Engineering
in Energy Technology and Management

The Joint Graduate School of Energy and Environment
at King Mongkut's University of Technology Thonburi

2nd Semester 2013

Thesis Committee

....
(Assoc. Prof. Dr. Suneerat Fukuda   )   Advisor

....
(Assoc. Prof. Dr. Navadol Laosiripojana)   Member

....
(Asst. Prof. Dr. Prasert Reubroycharoen)   Member

....
(Assoc. Prof. Dr. Phavanee Narataruksa)   External Examiner

Thesis Title: Upgrading of Pyrolysis Bio-Oil by Catalytic Deoxygenation Using CoMo and NiMo based Catalysts.

Student's name, organization and telephone/fax numbers/email

Ms. Siyada Iangmee

The Joint Graduate School of Energy and Environment (JGSEE)

King Mongkut's University of Technology Thonburi (KMUTT)

126 PrachaUthit Rd., Bangmod, Tungkru, Bangkok 10140 Thailand

Telephone: 0-8847-62007

Email: i_siyada@hotmail.com

Supervisor's name, organization and telephone/fax numbers/email

Assoc. Prof. Dr. Suneerat Fukuda

The Joint Graduate School of Energy and Environment (JGSEE)

King Mongkut's University of Technology Thonburi (KMUTT)

126 PrachaUthit Rd., Bangmod, Tungkru, Bangkok 10140 Thailand

Telephone: 0-8976-15712 or 02-470-8309-10 Ext. 4148

Email: suneerat@jgsee.kmutt.ac.th

Topic: Upgrading of Pyrolysis Bio-Oil by Catalytic Deoxygenation Using CoMo and NiMo based Catalysts.

Name of student: Ms. Siyada Iangmee   **Student ID:** 54910429

Name of Supervisor: Assoc. Prof. Dr. Suneerat Fukuda

ABSTRACT

Bio-oil produced from the fast pyrolysis of biomass is a potential candidate to replace conventional fossil-derived fuels. The fast pyrolysis derived oil generally has high oxygen contents (30-40 % wt) that make it unstable, corrosive and have low heating value. Because of unstable properties of bio-oil, a model bio-oil, which is the mixture of pure chemicals mainly present in real bio-oil, was used in this study. This study aims to investigate the upgrading of model bio-oil by deoxygenation method for oxygen removal using various catalysts. The composition of model bio-oil used resembles that derived from pyrolysis of eucalyptus bark, which is well known as major residue from paper production. The experiments were done in a high-pressure autoclave reactor operated on a batch mode with CoMo and NiMo based catalysts. The effects of stirring rate, operating temperature, catalyst type and dosage, initial pressure of H_2 and presence of water on oxygen removal performance from bio-oil and properties of upgraded bio-oil products were investigated.

At 350°C, solid formation and oil cracking were observed from experiments using the CoMo catalyst, which resulted in a low yield of the upgraded oil product and low deoxygenation efficiency. The operating temperature of 325°C was then used as the maximum temperature in all further experiments. The results illustrate that increasing the stirring rate to 1000 rpm could minimize the mass transfer limitation and also increased the efficiency of oxygen removal at temperature range of 250-325°C. NiMo catalyst gave higher deoxygenation efficiency throughout the temperature range of 275-325°C compared to CoMo catalysts. Initial pressure of H_2 was another factor that affects deoxygenation efficiency. The higher the initial pressure, the higher the deoxygenation efficiency. The presence of water in bio-oil was also found to inhibit the oxygen removal performance of catalysts.

ACKNOWLEDGEMENTS

CONTENTS

CONTENTS (Cont')

LIST OF TABLES

LIST OF FIGURES

LIST OF FIGURES (Cont')

CHAPTER 1

INTRODUCTION

1.1 Rationale

The demands of transportation fuel increase continuously, while the amount of fossil fuel distinctly decreases. This problem leads to negative effects on global energy security and economic issue in the countries which import fossil fuel. Because of the limited resources, renewable resources are potentially good alternatives for conventional fossil-derived fuels and biomass is the only resource that can be used for the production of liquid transportation fuels.

Thailand is an agricultural country and generates a lot of waste from agricultural production and the agro-processing industry. A lot of purpose-grown crops are also the other potential biomass source. Lignocellulosic biomass can be used as feedstocks for bio-oil production by fast pyrolysis process. The product bio-oil is a dark brown liquid which is a complex mixture of condensed water and organic compounds such as ketones, aldehydes, alcohols, furans, acids, phenols etc. The high oxygen content in bio-oil gives negative effects to oil properties, including oil instability, high acidity and low heating value. Therefore, upgrading to reduce oxygen content in bio-oil is necessary before use as liquid fuels especially in automotive engines.

This study proposes the catalytic deoxygenation for bio-oil upgrading. Various types of commercial catalysts were tested on model bio-oil. The selected biomass feedstock for bio-oil production is eucalyptus bark, which is one of the wastes from the pulp and paper industry, and an energy crop for Thailand. The experiments were carried out using a lab-scale high pressure autoclave operated on a batch mode. The effect of catalysts and operating conditions (i.e. pressure, temperature and time), as well as properties of bio-oil (i.e. moisture content and composition) on the characteristics of the upgraded products especially oxygen content were investigated.

1.2 Literature Review

1.2.1 Eucalyptus as a Potential Biomass for Bio-Oil Production

The potential of biomass is very important for the selection of biomass for a sustainable bioenergy project. The data and information about biomass quantity and utilization in Thailand from the agricultural sector in 2006 and 2007 and the Department of Alternative Energy Development and Efficiency (DEDE) in 2007 showed that the highest potential biomass was fast growing trees grown particularly for energy production. Eucalyptus is one of fast glowing tree member in DEDE project. Besides, DEDE concluded that biomass waste from paper industry that is eucalyptus bark is suitable raw material for fuel production. This is because a large amount of eucalyptus bark was produced from this industry (Department of Alternative Energy Development and Efficiency, 2011). Furthermore, eucalyptus has been found in a previous study (Yuenyongchaiwat, 2010) to give high bio-oil yield comparing with other biomass feedstocks. In the study by Yuenyongchaiwat, bio-oil is produced by pyrolysis in a lab-scale vacuum pyrolysis system operated on a batch mode. The selected biomass feedstocks include rice straw, eucalyptus bark/root, rice husk, rubber wood and Shorea obtuse. The results showed that the maximum bio-oil yields were obtained at different pyrolysis temperatures depending on the type of biomass and eucalyptus gave the highest bio-oil yield.

1.2.2 Upgrading of Oil from Plant and Bio-Oil by Catalytic Deoxygenation

The oxygen contents in bio-oil composition make it different from conventional fossil oils that is the main problem for direct utilization. Therefore, previous studies mainly focus on upgrading processes by reducing the oxygen content.

Toba et al. (2011) studied hydrodeoxygenation activities on waste cooking oil by using $NiMo/Al_2O_3$ (NiO: 3.7 wt%, MoO_3: 14.0 wt%) and NiW/Al_2O_3 (NiO: 4.2 wt%, MoO_3: 29.0 wt%) to compare with $CoMo/Al_2O_3$ (CoO: 3.7 wt%, MoO_3: 14.0 wt%) catalysts. All catalysts were sulfided in the stream of 5% H_2S/H_2 gas at 360°C for 3 h before reaction. The reaction was carried out in a batch reactor, a swing type stainless steel autoclave reactor at temperature 350°C and pressure 7 MPa for 3 h. The results showed that No and NiW catalysts are more suitable for hydrodeoxygenation of waste cooking oils than is the CoMo catalyst because NiMo and NiW catalysts showed high hydrodeoxygenation activity and gave hydrocarbons with high yield.

Payormhorm et al. (2010) improved the quality of the bio-oil obtained from the pyrolysis of Leucaena leucocephala, rice straw, algae and sawdust via deoxygenation catalyzed by platinum supported on alumina (Pt/Al_2O_3) under nitrogen atmosphere. The results indicated that bio-oil from pyrolysis of algae gave the highest % oxygen removal, ca. 81.5%. The composition of deoxygenated bio-oil analyzed by using GC-MS also indicated that the bio-oil derived from pyrolysis of algae consisted of nitrogen compounds and a small amount of phenol derivatives. These were easier to be removed than the more complicated oxygenated compounds found in bio-oils generated from pyrolysis of Leucaena leucocephala and sawdust.

1.2.3 Model Bio-Oil Used in Catalytic Deoxygenation

Due to the unstable properties of real bio-oil, to control the same properties of bio-oil reactants in each upgrading experiment is very difficult. Thus, a chemical or the mixture of chemicals which is chosen from the main compounds in real bio-oil is typically used as the model bio-oil to simulate the catalytic deoxygenation in the previous studies.

Senol et al. (2005) eliminated oxygen in carboxylic groups with model compounds of methyl heptanoate and methyl hexanoate on sulphidedNiMo/c-Al_2O_3 and CoMo/c-Al_2O_3 in a flow reactor to discern the reaction schemes. Aliphatic methyl esters produced hydrocarbons via three main pathways: the first pathway gave alcohols followed by dehydration to hydrocarbons. The de-esterification yielded an alcohol and a carboxylic acid in the second pathway. Carboxylic acid was further converted to hydrocarbons either directly or with an alcohol intermediate.

Gutierrez et al. (2009) studies on zirconia-supported mono- and bimetallic noble metal (Rh, Pd, Pt) catalysts showed these catalysts to be active and selective in the hydrogenation of guaiacol (GUA) at 100 °C and in the hydrodeoxygenation of GUA at 300°C. GUA was used as model compound for wood-based pyrolysis oil. At the temperatures tested, the performance of the noble metal catalysts, especially the Rh-containing catalysts was similar or better than that of the conventional sulfide CoMo/Al_2O_3 catalyst. The carbon deposition on the noble metal catalysts was lower than that on the sulfidedCoMo/Al_2O_3 catalyst. The performance of the Rh-containing catalysts in the reactions of GUA at the tested conditions demonstrates their potential in the upgrading of wood-based pyrolysis oils.

Fisk et al. (2009) studied the deoxygenation of model bio-oil over the supported platinum catalyst. Synthetic bio-oil samples, a mixture of methanol, acetaldehyde, acetic acid, glyoxal, acetol, glucose, guaiacol, furfural, vanillin and de-ionized water with respect to the main compound types and their concentration in typical pyrolysis oil, were used as the feedstocks. Upgrading experiments were performed in a stirred stainless steel autoclave. The results showed that supported platinum catalysts were found to show significant activity for the deoxygenation of a model bio-oil.

1.3 Research Objectives

To study the catalytic deoxygenation of model bio-oil by using various catalysts for oxygen removal

1.4 Scope of the Study

1. Characterization of bio-oil: Elemental analysis, calorific value, chemical compositions
2. Set-up of bio-oil catalytic deoxygenation experimental device: Stainless steel autoclave reactor
3. Investigation of the effect of operating conditions on the oxygen removal by catalytic deoxygenation using CoMo and NiMo based catalysts from model bio-oil having the same composition as bio-oil derived from pyrolysis of eucalyptus bark (Yuenyongchaiwat, 2010).
4. Characterization of products:
   a. Bio-oil composition : Elemental analysis and GC-MS analysis
   b. Gas composition: GC analysis.

CHAPTER 2

THEORIES

2.1 Biomass

Generally, biomass is the matter that can be derived directly or indirectly from plants and utilized as energy or materials in substantial amounts. "Indirectly" refers to the products available via animal husbandry and the food industry. Biomass is called as "phytomass" and is often translated bioresource or bio-derived-resource. The resource base includes hundreds of thousands of plant species, terrestrial and aquatic, various agricultural, forestry and industrial residues and process waste, sewage and animal wastes. Energy crops, which make the large scale energy plantation, will be one of the most promising biomass, though it is not yet commercialized at the present moment. Specifically biomass means wood, Napier grass, rape seed, water hyacinth, giant kelp, chlorella, sawdust, wood chip, rice straw, rice husk, kitchen garbage, pulp sludge, animal dung etc. As plantation type biomass, eucalyptus, hybrid poplar, oil palm, sugar cane, switch grass etc. are included in this category (The Japan Institute of Energy, 2008).

2.1.1 Chemical Composition in Biomass

Biomass is carbon-based and is composed of a mixture of organic molecules containing hydrogen, usually such as atoms of oxygen, often nitrogen and also small quantities of other atoms, including alkali, alkaline earth and heavy metals. These metals are often found in functional molecules such as the porphyrins which include chlorophyll which contains magnesium.

2.1.2 Plant Material

The carbon used to construct biomass is absorbed from the atmosphere as carbon dioxide (CO_2) by plant life, using energy from the sun. Plants may subsequently be eaten by animals and thus converted into animal biomass. However, the primary absorption is performed by plants. If plant material is not eaten, it is generally either broken down by microrganisms or burned.

- If broken down, it releases the carbon back to the atmosphere, mainly as either carbon dioxide (CO_2) or methane (CH_4), depending upon the conditions and processes involved.

- If burned, the carbon is returned to the atmosphere as CO_2.

These processes have happened for as long as there have been plants on Earth and is part of what is known as the carbon cycle, as show in Figure 2.1.
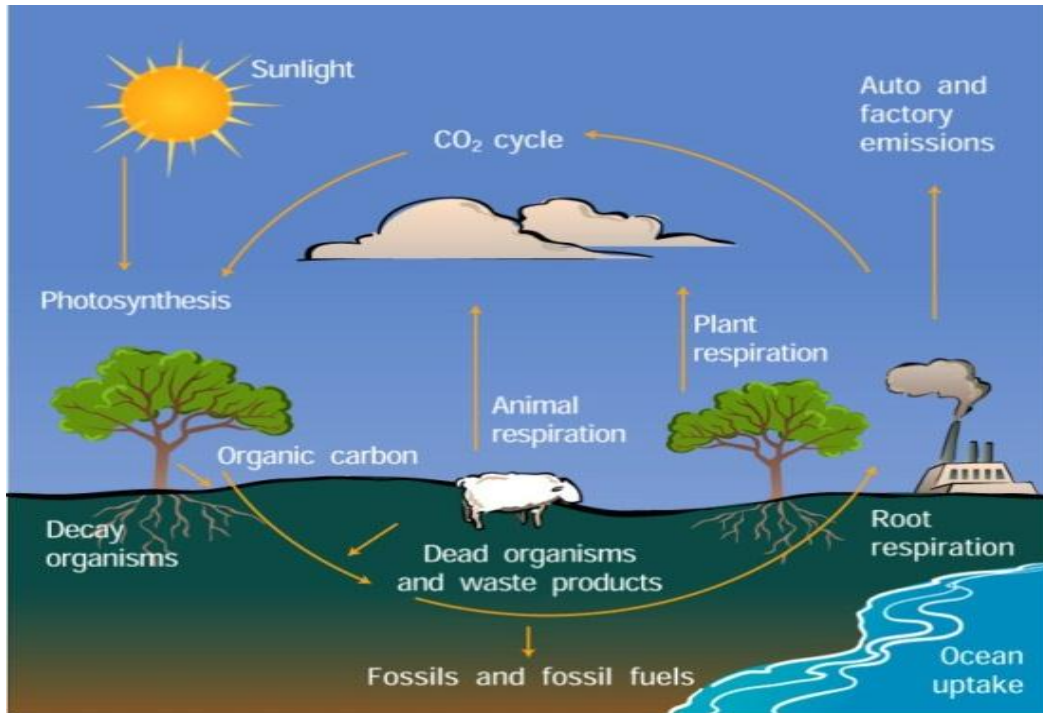
Figure2.1 The carbon cycle (The Japan Institute of Energy, 2008).

2.2 Biomass to Fuels

Biomass is a renewable source generated by plants through the process of photosynthesis with energy being provided by the sun. Wood is the oldest form of biomass fuel known to mankind, and was used for centuries for heating and cooking; indeed, wood is still used for these purposes in the developing world. Transportation and storage of biomass is not easy because of its bulkiness and degradation. It is, therefore, reasonable to use biomass in the areas where it is produced. For this reason, biomass is used in or nearby regions where biomass supply and demand are balanced. However, when biomass is converted into more transportable form like pellet or liquid fuels, it can be utilized in distant regions (The Japan Institute of Energy, 2008).

2.3 Pyrolysis

Pyrolysis is the precursor to gasification, and takes place as part of both gasification and combustion. It consists of thermal decomposition in the absence of oxygen. It is essentially based on a long established process, being the basis of charcoal burning. Pyrolysis is the precursor to gasification, and takes place as part of both gasification and combustion. It consists of thermal decomposition in the absence of oxygen. It is essentially based on a long established process and is the basis of charcoal burning. The products of pyrolysis include gas, liquid and a sold char, with the proportions of each depending upon the parameters of the process. The products and application of these thermal conversion processes are summarized in Figure 2.2.
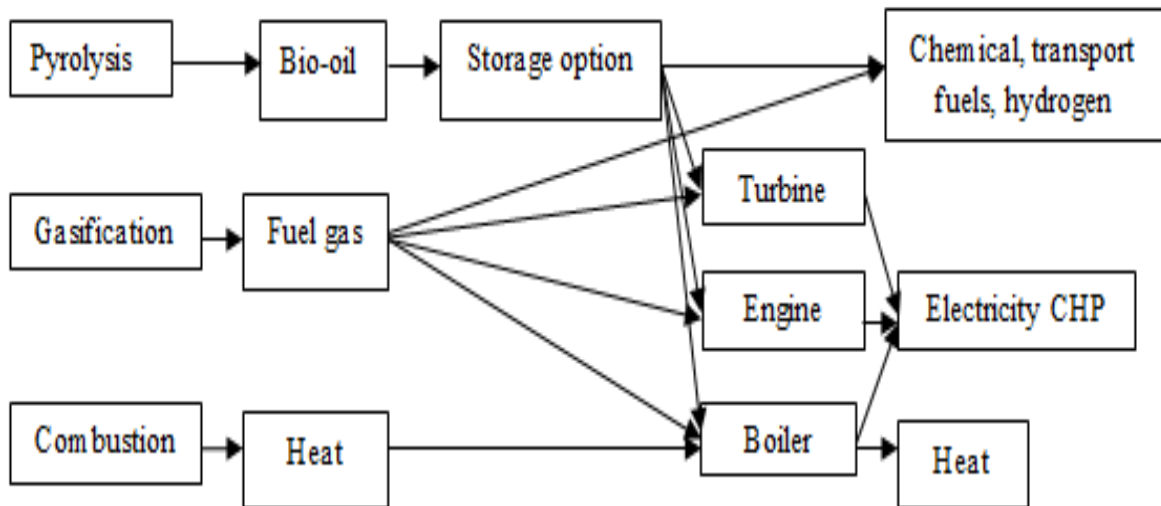
Figure 2.2 Products from thermal biomass conversion. (Horgan, et al., 1992)

2.3.1 Theory of Pyrolysis (Horgan et al., 1992)

Biomass fuels and residues can be converted into energy via thermal, biological and physical processes. In thermal conversion, combustion is already widely practiced, while gasification attracts a lot of interest due to its potential for high overall efficiencies as compared to combustion. Fast pyrolysis is also interesting as the liquid fuel product offers advantages in storage, transport and versatility in applications, although it is still at relatively early stage of development.

Combustion is widely practiced wherever economically justified. The product can only satisfy the heat market directly or power production via a Rankin cycle something similar. Efficiencies are low at small capacities and fouling and emissions are problematic

in many applications. Gasification offers higher efficiencies of operation, and while on the verge of being fully commercial still requires demonstration at commercially attractive scales of operation. Fast pyrolysis for liquid offers the advantage of liquid that can be stored and/or transported to offer a more versatile optimized system. The bio-oil can also be used as an energy carrier and as a source of chemicals.

Lower process temperatures and longer vapor residence times favor the production of charcoal. High temperature and longer residence time increase the biomass conversion to gas while moderate temperature and short vapor residence time are optimum for producing liquids. Table 2.1 indicates the product distribution obtained from different modes of pyrolysis process. Fast Pyrolysis for liquids production is of particular interest currently.

Table 2.1 Typical product yields (dry wood basis) obtained by different modes of pyrolysis of wood (Horgan et al., 1992).

Process	Conditions	Liquid	Char	Gas
Fast Pyrolysis	Moderate temperature, short residence time, particularly vapor	75%	12%	13%
Carbonization	Low-temperature, very long residence time	30%	35%	35%
Gasification	High temperature, long residence times	5%	10%	85%

Fast pyrolysis occurs within a few seconds or less. Therefore, not only chemical reaction kinetics, but also heat and mass transfer processes, as well as phase transition phenomena, play important roles. The critical issue is to bring the reacting biomass particle to the optimum process temperature and minimize its exposure to the intermediate (lower) temperatures that favor the formation of charcoal. One way to achieve this objective is by using small particles, for example in the fluidized bed processes. Another possibility is to transfer heat very fast only to the particle surface that contacts the heat source.

The general changes that occur during pyrolysis are enumerated below.

(1) Heat transfer from a heat source to increase the temperature inside the fuel;

(2) The initiation of primary pyrolysis reactions at this higher temperature releases volatiles and forms char;

(3) The flow of hot volatiles toward cooler solids results in heat transfer between hot volatile and cooler un-pyrolyzed fuel;

(4) Condensation of some volatiles in the cooler parts of the fuel, followed by secondary reactions, can produce tar;

(5) Autocatalytic secondary pyrolysis reactions proceed while primary pyrolytic reactions simultaneously occur in competition; and

(6) Further thermal decomposition, reforming, water gas shift reactions, radical recombination, and dehydration can also occur, which are the function of the process's resident time/temperature/pressure profile.

Pyrolysis may be conventional or fast pyrolysis, depending on operating conditions that are used. Conventional pyrolysis may also be termed slow pyrolysis. The term "slow pyrolysis" and "fast pyrolysis" are somewhat arbitrary and have no precise definition of the times or heating rates involved in each. Many pyrolysis runs have been performed at rates that are not considered fast or slow but are conducted in a broad range between these extremes.

2.3.2   Slow Pyrolysis

Slow pyrolysis has been used for the production of charcoal. Slow pyrolysis is a thermo-chemical decomposition of organic material at elevated temperatures in the absence of oxygen. Approximately 35% by weight of the dry feed material is converted to a high-carbon char material. The heating rate in conventional pyrolysis is typically much slower than that used in fast pyrolysis. A feedstock can be held at constant temperature or slowly heated. Vapors can be continuously removed as they are formed.

2.3.3   Fast Pyrolysis

Fast pyrolysis is a high temperature process in which biomass is rapidly heated in the absence of oxygen. As a result, it decomposes to generate mostly vapours and aerosols, and some charcoal. Liquid production requires very low vapour residence time to minimize secondary reactions of typically 1 s, although acceptable yields can be obtained at residence times of up to 5 s if the vapour temperature is kept below $400^{o}C$. After cooling and condensation, a dark brown mobile liquid is formed which has a heating value about half that of conventional fuel oil. While it is related to the traditional pyrolysis processes for making charcoal, fast pyrolysis is an advanced process which is carefully controlled to give high yields of liquid. Research has shown that maximum liquid yields are obtained

with high heating rates, at reaction temperatures around 500°C and with short vapour residence times to minimize secondary reactions. These utilize very short vapour residence times of between 30 and 1500 ms and reactor temperatures around 500°C. Both residence time and temperature control is important to "freeze'" the intermediates of most chemical interest in conjunction with moderate gas/vapour phase temperatures of 400±500°C before recovery of the product to maximize organic liquid yields.
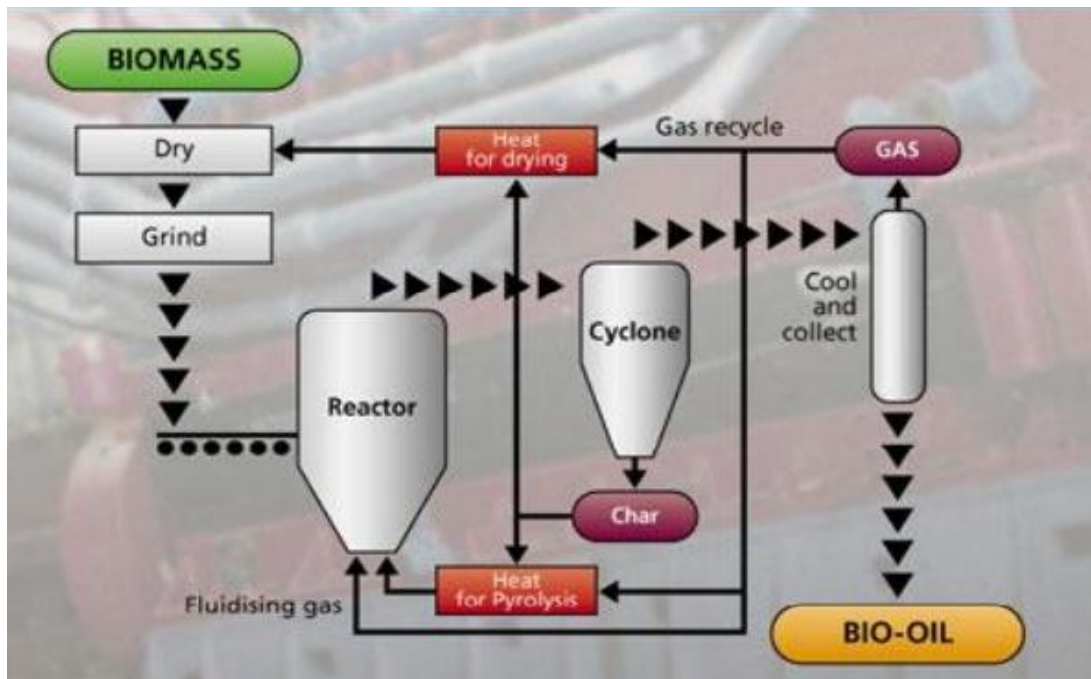
Figure 2.3 Biomass Pyrolysis Cycle (Bridgwater, 2002)

2.4 Bio-Oil (Oasmaa et al., 1999)

The liquid product from biomass pyrolysis is known as biomass pyrolysis oil, or bio-oil, pyrolysis oil, or bio-crude for short. Bio-oil is not a product of thermodynamic equilibrium during pyrolysis but is produced with short reactor times and rapid cooling or quenching from the pyrolysis temperatures. This produces a condensate that is also not at thermodynamic equilibrium at storage temperatures. The chemical composition of the bio-oil tends to change toward thermodynamic equilibrium during storage.

2.4.1　Composition and Physicochemical Properties of Bio-Oil

Bio-oils are multi-component mixtures of different sized molecules derived from depolymerization and fragmentation of cellulose, hemicellulose and lignin. Therefore, the elemental composition of bio-oil and petroleum derived fuel is different, and the basic data are shown in Table 2.2.

Table 2.2 Typical properties of wood pyrolysis bio-oil and heavy fuel oil (Oasmaa et al., 1999)

Physical property	Bio-oil	Heavy fuel oil
Moisture content (wt%)	15–30	0.1
pH	2.5	-
Specific gravity	1.2	0.94
Elemental composition (wt%)		
C	54–58	85
H	5.5–7.0	11
O	35–40	1.0
N	0–0.2	0.3
Ash	0–0.2	0.1
HHV (MJ/kg)	16–19	40
Viscosity (at 50 °C) (cP)	40–100	180
Solids (wt%)	0.2–1	1
Distillation residue (wt%)	up to 50	1

2.4.2　Water

Bio-oil has a content of water as high as 15–30 wt% derived from the original moisture in the feedstock and the product of dehydration during the pyrolysis reaction and storage. The presence of water lowers the heating value and flame temperature, but on the other hand, water reduces the viscosity and enhances the fluidity, which is good for the atomization and combustion of bio-oil in the engine. Shihadeh and Hochgreb compared the bio-oils of NREL (National Renewable Energy Laboratory, US) to those of ENSYN (Ensyn Technologies, Inc., CA), and found that additional thermal cracking improved its chemical and vaporization characteristics. The better performance and better ignition of NREL oil derived from its lower water content and lower molecular weight.

2.4.3 Oxygen

The oxygen content of bio-oils is usually 35–40% (Diebold et al., 2001) distributed in more than 300 compounds, depending on the resource of biomass and severity of the pyrolytic processes (temperature, residence time and heating rate). The presence of oxygen creates the primary issue for the differences between bio-oils and hydrocarbon fuels. The high oxygen content leads to the lower energy density than the conventional fuel by 50% and immiscibility with hydrocarbon fuels also. In addition, the strong acidity of bio-oils makes them extremely unstable. Because of their complex compositions, bio-oils show a wide range of boiling point temperature. During the distillation, the slow heating induces the polymerization of some reactive components, and bio-oils start boiling below 100 °C, while stopping at 250–280 °C, leaving 35–50 wt% as solid residues. Therefore, bio-oils cannot be used in the instance of complete evaporation before combustion.

2.4.4 Viscosity

Depending on the biomass feedstocks and pyrolytic processes, the viscosities of bio-oils vary over a large range. Bio-oils (Oasmaa et al., 1999) produced from Pterocarpusindicus and Fraxinusmandshurica had a kinetic viscosity of 70–350 mPa s and 10–70 mPa s, respectively, and that from rice straw had a minimum kinetic viscosity of about 5–10 mPa s for its high water content. Sipilae` et al. (1998) investigated the bio-oils from hardwood, softwood and straw by flash pyrolysis in an atmospheric fluidized bed. It was found that the viscosities were reduced in the bio-oils with higher water content and less water insoluble components. Viscosity was also affected by alcohols: an addition of 5 wt% methanol into hardwood pyrolysis oil with low methanol content decreased its viscosity by 35%. The straw oil is less viscous and had the highest methanol content of 4 wt%.

The research of NREL (Diebold, 2005) showed that the viscosity increased only from 20 to 22 cP over a 4 month period when stored at 20 °C with 10% methanol addition to the bio-oil. This would extrapolate to a viscosity of 30 cP after storage for 12 months. Ethanol at 20% had a similar stabilizing effect. With 10viscosity at 40 °C rose from about 13 cP to an interpolated 15 cP after preheating for 12 h at 90 °C, e.g. to reduce the viscosity for ease of atomization.

Boucher et al. (2000) tested bio-oil performance with the addition of methanol regarding its use as a fuel for gas turbine applications. The methanol reduced the density

and viscosity and increased the stability with the limitation of a lowered flash point in the blend.

2.4.5   Acidity

Bio-oils are comprised of substantial amounts of carboxylic acids, such as acetic and formic acids, which leads to low pH values of 2–3. The bio-oil of pine had a pH of 2.6, while that of hardwood was 2.8 (Sipilae` et al., 1998). Acidity makes bio-oil very corrosive and extremely severe at elevated temperature, which imposes more requirements on construction materials of the vessels and the upgrading process before using bio-oil in transport fuels.

2.4.6   Heating Value

The properties of bio-oils depend on factors, such as biomass feedstocks, production processes, reaction conditions and collecting efficiency. Usually the bio-oils of oil plants have a higher heating value than those of straw, wood or agricultural residues. Beis et al. (2000) conducted pyrolysis experiments on samples of safflower seed and obtained bio-oil with a heating value of 41.0 MJ/kg and a maximum yield of 44%. Ozcimen et al., (2004) produced bio-oil from rapeseed cake in a fixed bed with a heating value of 36.4 MJ/kg and a yield of 59.7%. However, taking wood and agricultural residues as raw materials, the bio-oils have a heating value of about 20 MJ/kg and a yield up to 70–80%.

2.4.7   Ash

The presence of ash in bio-oil can cause erosion, corrosion and kicking problems in the engines and the valves, and even deterioration when the ash content is higher than 0.1 wt%. However, alkali metals are problematic components of the ash. More specifically, sodium, potassium and vanadium are responsible for high temperature corrosion and deposition, while calcium is responsible for hard deposits. The H50 bio-oil was found to contain 2 ppm K, 6 ppm Na and 13 ppm Ca (Boucher et al., 2000) The best job of hot gas (Ozcimen et al., 2004) filtering to date at NREL (Scahill et al., 1996) resulted in less than 2 ppm alkali metals and 2 ppm alkaline earth metals in the bio-oil.

2.5 Composition of Bio-Oil Derived from Pyrolysis of Eucalyptus Bark

The 99.7% of bio-oil, a complex mixture containing carbon, hydrogen and oxygen, is composed of acids, alcohols, aldehydes, esters, ketones, sugars, phenols, guaiacols, syringols, furans, lignin derived phenols and extractible terpene with multi-functional groups (Guo et al., 2001).

Yuenyongchaiwat P. (2010) studied the bio-oil production by pyrolysis process in the year 2010, and the compositions of bio-oil are used as in Table2.3. There functional group could be identified including ketone, furan, phenolic, carboxylic acid, ester, halo-alkane, amine, hydroxyl, aldehyde, alkene, toluene derivative, benzoquinone derivative and aldehyde. The main functional groups of eucalyptus oil include ketone (26.05%), phenolic (25.00%) and furan (8.56%). For rice straw, ketone (38%), furan (11.42%) and hydroxyl (8.13%) were the major group. In conclusion, bio-oils are a complex mixture, highly oxygenated with a great amount of large size molecules, which nearly involve all species of oxygenated organics,such as esters, ethers, aldehydes, ketones, phenols, carboxylicacids and alcohols (Peng et al., 2000).

Table 2.3 GC-MS analysis of bio-oil products from pyrolysis of Eucalyptus (Yuenyongchaiwat, 2010).

Chemical name	Retention time (min)	%Area Eucalyptus
1-Hydroxy-2-propanone	2.16	9.06
1-Hydroxy-2-butanone	3.33	6.23
4-Hydroxy-4-methyl-2-pentanone	4.78	3.41
2-Hydroxy-2-cyclopenten-1-one	7.23	5.16
2-Hydroxy-3-methyl-2-cyclopenten-1-one	11.19	2.19
Total of ketone		26.05
Furfural	4.58	4.61
2-Furanmethanol	5.17	1.39
2,5-Dimethoxytetrahydrofuran	6.31	0.32
Dihydro-2(3H)-Furanone	6.84	0.78
2(5H)-Furanone	6.91	1.46
Total of furan		8.56
Phenol	9.57	0.65
3-Methyphenol	13.54	1.1
2-Methoxyphenol	13.87	2.88
2-Methoxy-4-methylphenol	18.55	1.13
1,2-Benzenediol	19.3	0.72
3-Methoxy-1,2-Benzenediol	21.65	1
2-Methoxybenzeneethanol	22.39	1.79
2-Methoxy-4-vinylphenol	23.92	2.13
2,6-Dimethoxyphenol	25.56	8.36
2,6-Dimethyl-4-(2-propenyl)phenol	39.32	5.24
Total of phenolic		25
3,5-Dimethoxy-4-hydroxyphenylacetic acid	41.9	1
Propanoic acid	2.42	0.72
Total of carboxylic acid		1.72
2-Propenyl ester butanoic acid	4.54	0.58
Total of ester		0.58
3-Methyliminoperhydro-1,3-oxazine	9.99	1.35
2-Propanamine	14.05	5.43
Total of amine		6.78
2,3-Dihyro-1,1-dimethyl-3-oxo-5-(trifluoromethyl)-1H-pyrazolium hydroxide	34.27	6.48
Total of hydroxy		6.48
Propanal	3.51	5.39
Total of aldehyde		5.39
2-(2-Naphthyl)-1-propene	29.58	6.92
Total of alkene		6.92
2,3,5-Trimethoxytoluene	32.78	2.09
Total of toluene derivative		2.09
3-(3',5'-Dimethoxy-4'-hydroxyphenyl)-E-2-propenal	48.82	0.32
Total of aldehyde		0.32

2.6 Upgrading of Bio-Oil

The deleterious properties of high viscosity, thermal instability and corrosiveness present many obstacles to the substitution of fossil-derived fuels by bio-oils. So, an upgrading process by reducing the oxygen content is required before its application. The recent upgrading techniques are described as follows.

2.6.1   Hydrodeoxygenation (HDO)

The hydro-process is performed in hydrogen providing solvents activated by the catalysts of Co–Mo, Ni–Mo and their oxides or loaded on Al_2O_3 under pressurized conditions of hydrogen and/or CO. In these catalysts, Co or Ni serves as promoters, donating electrons to the molybdenum atoms. This weakens the bond between molybdenum and sulfur, and thereby generates a sulfur vacancy site. These sites are the active sites in both HDS and HDO reactions (Massoth et al., 2006; Ryymin, 2010; Badawi et al., 2011; Topsoe et al., 1996).

Romero et al. (2010) studied HDO of 2-ethylphenol on MoS_2-based catalysts and proposed the reaction mechanism depicted in Figure 2.4. The oxygen of the molecule is believed to adsorb on a vacancy site of a MoS_2 slab edge, activating the compound. S-H species will also be present along the edge of the catalyst as these are generated from the H_2 in the feed. This enables proton donation from the sulfur to the attached molecule, which forms a carbocation. This can undergo direct C-O bond cleavage, forming the deoxygenated compound, and oxygen is hereafter removed in the formation of water.
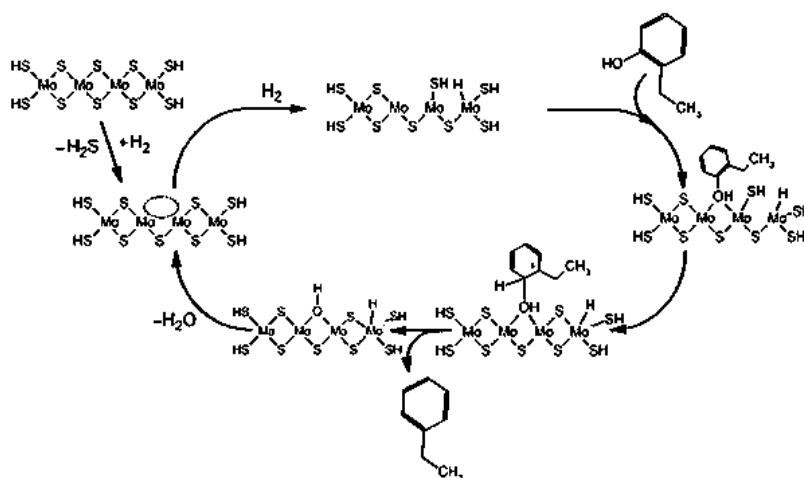
Figure 2.4 Proposed mechanism of HDO of 2-ethylphenol over a Co-MoS2 catalyst. The dotted circle indicates the catalytically active vacancy site. The figure is drawn on the basis of information from Romero et al., (2010).

For the mechanism to work, it is a necessity that the oxygen group formed on the metal site from the deoxygenation step is eliminated as water. During prolonged operation it has been observed that a decrease in activity can occur due to transformation of the catalyst from a sulphide form toward an oxide form. In order to avoid this, it has been found that co-feeding H_2S to the system will regenerate the sites and stabilize the catalyst (Senol, 2007; Senol, 2007; Ryymin, 2009; Badawi, 2009). However, the study of Senol et al. (2007) showed that trace amounts of thiols and sulphides were formed during the HDO of 3 wt% methyl heptanoate in m-xylene at 15 bar and 250 ˚C in a fixed bed reactor with $Co\text{-}MoS_2/Al_2O_3$co-fed with up to 1000 ppm H_2S. Thus, these studies indicate that sulfur contamination of the otherwise sulfur free oil can occur when using sulphide type catalysts. An interesting perspective in this is that $Co\text{-}MoS_2/Al_2O_3$is used an industrial HDS catalyst where it removes sulfur from oil down to a level of a few ppm (Prins, 2008). On the other hand, Christensen et al. (2009) showed that, when synthesizing higher alcohols from synthesis gas with $Co\text{-}MoS_2/C$ co-fed with H_2S, thiols and sulfides were produced as well. Thus, the influence of the sulfuron this catalyst is difficult to evaluate and needs further attention.

On the basis a density functional theory (DFT) calculations, Moberg et al. (2010) proposed MoO_3as catalyst for HDO. These calculations showed that the deoxygenation on MoO_3 occurs similar to the path in Figure 2.4, i.e. chemisorption on a coordinatevely unsaturated metal site, proton donation, and desorption. For both oxide and sulphide type catalysts the activity relies on the presence of acid sites.

The initial chemisorption step is a Lewis acid/base interaction, where the oxygen lone pair of the target molecule is attracted to the unsaturated metal site. For this reason, it can be speculated that the reactivity of the system must partly rely on the availability and strength of the Lewis acid sites on the catalyst. Gervasini et al. (1991) reported that the relative Lewis acid site surface concentration on different oxides is:

$$Cr_2O_3 > WO_3 > Nb_2O_5 > Ta_2O_5 > V_2O_5 \approx MoO_3 \qquad (2.1)$$
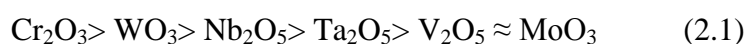
This should be matched against the relative Lewis acid site strength of the different oxides. This was investigated by Li and Dixon, where the relative strengths were found to be:

$$WO_3 > MoO_3 > Cr_2O_3 \qquad (2.2)$$

The subsequent step of the mechanism is proton donation. This relies on hydrogen available on the catalyst, which for the oxides will be present as hydroxyl groups. To have

the proton donating capabilities, Brønsted acid hydroxyl groups must be present on the catalyst surface. In this context the work of Busca showed that the relative Brønsted hydroxyl acidity of different oxides is (Moberg, 2010):

$$WO_3 > MoO_3 > V_2O_5 > Nb_2O_5 \qquad (2.3)$$
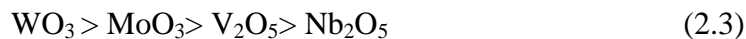
The trends of Equations 2.1-2.3 in comparison to the reaction path of deoxygenation reveals that MoO_3 functions as a catalyst due to the presence of both strong Lewis acid sites and strong Brønsted acid hydroxyl sites. However, Whiffen and Smith (2010) investigated HDO of 4-methylphenol over unsupported MoO_3 and MoS_2 in a batch reactor at 41-48 bar and 325-375 °C, and found that the activity of MoO_3 was lower than that for MoS_2 and that the activation energy was higher on MoO_3 than on MoS_2 for this reaction. Thus, MoO_3 might not be the best choice of an oxide type catalyst, but on the basis of Eqs. 2.8-2.10 other oxides seem interesting for HDO.

Specifically, WO_3 is indicated to have a high availability of acid sites. Echeandia et al. (2010) investigated oxides of W and Ni-W on active carbon for HDO of 1 wt% phenol in n-octane in a fixed bed reactor at 150-300°C and 15 bar. These catalysts were all proven active for HDO, and especially, the Ni-W system had potential for the complete conversion of the model compound. Furthermore, a low affinity for carbon was observed during the 6 h of experiments. This low value was ascribed to a beneficial effect from the non-acidic carbon support.

2.6.2 Catalytic Cracking of Pyrolysis Vapors

Oxygen containing bio-oils are catalytically decomposed into hydrocarbons with the removal of oxygen as H_2O, CO_2 or CO. Nokkosmaki et al. (2000) proved ZnO to be a mild catalyst on the composition and stability of bio-oils in the conversion of pyrolysis vapors, and the liquid yields were not found to be substantially reduced. Although it had no effect on the water insoluble fraction (lignin derived), it decomposed the diethyl insoluble fraction (water soluble an hydro sugars and polysaccharides). After heating at 80 °C for 24 h, the increase in viscosity was significantly lowered for the ZnO-treated oil (55% increase in viscosity) as compared to the reference oil without any catalyst (129% increase in viscosity). Despite the indicated deactivation of the catalyst, the improvement in the stability of the ZnO treated oil was clearly observed. Adam et. Al. illustrated the effects and catalytic properties of Al-MCM-41, Cu/Al-MCM-41 and Al-MCM-41 with pores enlarged on bio-oil upgrading. The resulting compositions of vapors were changed through

the catalysts layer. Levoglucosan was completely eliminated, which was typical for each catalyst. While the catalysis increased the yields of acetic acid, furfural and furans, it reduced those of large molecular phenols among the cellulose pyrolysis products of spruce wood. The pore size enlargement and incorporation of catalysts reduced the yield of acetic acid and water.

Adjaye et al. (1995) studied the catalytic performance of the different catalysts for the upgrading of bio-oil. Among the five catalysts studied, HZSM-5 was the most effective catalyst for producing the organic distillate fraction, overall hydrocarbons and aromatic hydrocarbons and the least coke formation. Reaction pathways were postulated that bio-oil conversion proceeded as a result of thermal effects followed by thermo catalytic effects. The thermal effects produced separation of the bio-oil into light organics and heavy organics and polymerization of the bio-oil to char. The thermo catalytic effects produced coke, tar, gas, water and the desired organic distillate fraction.

Guo et al. (2003) reviewed various catalysts used in bio-oil, upgrading in detail and believed that although catalytic cracking is a predominant technique, the catalyst with good performance of high conversion and little coking tendency is demanding much effort. Although catalytic cracking is regarded as a cheaper route by converting oxygenated feedstock to lighter fractions, the results seem not promising due to high coking (8–25 wt%) and poor quality of the fuels obtained.

2.6.3 Emulsification

The simplest way to use bio-oil as a transport fuel seems to be to combine it directly with diesel. Although the bio-oils are immiscible with hydrocarbons, they can be emulsified by the aid of a surfactant. Chiaramonti et al. (2003) prepared emulsified bio-oil by the ratios of 25, 50 and 75 wt% and found the emulsions were more stable than the original ones. The higher the bio-oil content, the higher the viscosity of the emulsion. The optimal range of emulsifier to provide acceptable viscosity was between 0.5% and 2%. In particular, the effect of the long term use of emulsions on the stainless steel engine and its subassemblies should be estimated.

Ikura et al. (2003) obtained light fractions of bio-oil by centrifugation and emulsified them in No. 2 Diesel by CANMET surfactant with ratios of 10, 20 and 30 wt% separately.The cost of producing stable emulsions were 2.6 cents/L for 10% emulsion, 3.4 cents/L for 20% emulsion and 4.1 cents/L for 30% emulsion separately. The bio-oil was

determined to have a cetane number of 5.6, which will decrease by 0.4 for each 10% concentration augmentation. The viscosity of 10–20 wt% emulsions was much lower than that of pure bio-oil, and their corrosiveness was about half of that of bio-oil alone. Emulsification does not demand redundant chemical transformations, but the high cost and energy consumption input cannot be neglected. The accompanying corrosiveness to the engine and the subassemblies is inevitably serious.

2.6.4   Steam Reforming

Hydrogen is a clean energy resource and very important in the chemical industry. The rising focus on reforming the water fraction of bio-oil looks promising. Production of hydrogen from reforming bio-oil was investigated by NREL (Wang et al., 1997; Wang et al., 1998) extensively, including the reactions in a fixed bed or a fluidized bed and studies of the reforming mechanisms on model compounds. The fixed bed used in the conventional reforming of natural gas or naphtha is not suitable in the lignin derived fraction of bio-oil because of its tendency to decompose thermally and form carbon deposits on the upper layer of the catalyst and in the reactor freeboard.

Czernik et al. (2002) obtained hydrogen in a fluidized bed reactor from the carbohydrate-derived fraction of wood pyrolysis oil with a yield of about 80% of theoretical, which corresponds to approximately 6 kg of hydrogen from 100 kg of wood used for pyrolysis. Commercial nickel catalysts showed good activity in processing biomass derived liquids and was readily regenerated (20 min to 2 h) by steam or CO_2 gasification after deactivation, which occurred during reforming. The commercial catalysts, designed for fixed bed applications, were susceptible to attrition in the fluidized bed. Consequently, they were entrained at a rate of 5%/day. The development of a fluidizable catalyst that has both high activity and mechanical strength at the conditions of the steam reforming process is needed and is being pursued.

Garcia et al. (2002) chose magnesium and lanthanum as support modifiers to enhance steam adsorption, when facilitates the carbon gasification, while cobalt and chromium additives were applied to alleviate the coke formation reactions, which modified the metal sites forming alloys with nickel, and possibly, reducing the crystallite size. More hydrophilic sites surrounding nickel crystallites were effective in extending the duration of the catalyst's activity. The catalyst deactivation upon steam reforming of complex bio-oils

occurs much faster than with natural gas or naphtha, but the catalyst can be efficiently regenerated by steam or CO_2 gasification.

Takanabe et al. (2004) completely converted acetic acid, the model compound, by steam reforming over Pt/ZrO_2 catalysts, and found a hydrogen yield close to thermodynamic equilibrium. Analysis showed that Pt was essential for the steam reforming to proceed, and ZrO_2 was needed to activate the steam, which was also active for oligomer precursor formation under the conditions investigated. The results illustrated that steam reforming took place at the $Pt–ZrO_2$ boundary, and that deactivation occurred when this boundary is blocked by oligomers.

2.7 Product Analysis

2.7.1. Element Analyzer (Yuenyongchaiwat, 2010)

Elemental analysis analyzes for carbon, hydrogen, nitrogen, oxygen, sulfur and chlorine. Process of elemental analysis:

1. Find Carbon and Hydrogen element by burning the sample.
2. Find nitrogen and sulfur by chemical process.
3. Oxygen is residue from analysis.

2.7.2. Gas Chromatography (GC) (Asphaug, 2013)

Chromatography is a separation method used to identify and quantify different species in a mixture. This is done by separation of the species in two phases, mobile and stationary phases. In this study, gas is used as the mobile phase, hence the name gas chromatography. The gases used in gas chromatography are N_2, He and H_2. Helium is expensive and H_2 can be dangerous and demands certain precautions. N_2 is therefore mostly used, because it is relatively cheap, but needs a purity of 99.99% (Greibrokk, 2005; Ravindranath, 1989).

The principle of chromatography is to separate the species through a column. The species mix with the phases differently according to their volatility and affinity to the stationary phase. The species that mostly mixes with the mobile phase will pass fastest through the tube, and those which mix with the stationary phase will pass the more slowly. The velocities of the species depend on the composition of the mobile and stationary phases and the temperature.

At the end of the tube, there is a detector that registers the species as they pass through. These detectors are mostly TCD (Thermal conductivity detector) and FID (Flame-ionization detector). The TCD can be used for both inorganic and organic compounds and is the oldest detector used in gas chromatography. The carrier gas flows through a heated filament and the gas cools the filament by absorbing heat. The filament is set to a temperature, and the temperature different over the filament is measured as electrical resistance by the detector. A problem with using the TCD is low sensitivity.

The FID is mostly used for organic compounds. The carrier gas is mixed with H_2 and is burned with excess of air. There is an electric voltage between the flame and the collector. During the burning, ions and free electrons are formed, and the current in the detector is proportional to the amount of gas burned.

During quantitative analyses, an internal or external standard is often used to compensate for variations in the amount of injected samples (Greibrokk et al., 2005). A known amount of the standard is added to the sample. The ratio of added and measured amount of the standard is used to adjust the measured amount of the other species in the sample. The specie used as a standard has to be stable and not previously present in the sample. It also needs to be pure and have a retention time which is close to the other species in the sample (Greibrokk et al., 2005).

2.7.3. Gas Chromatography Mass Spectrometry (GC/MS) (Bridgwater, 2002)

A mass spectrometer can be defined as any instrument capable of producing ions from neutral species and provides a means of determining the mass of those ions, based on the mass-to-charge ration (*m/z*, where *z* is the number of elemental charges) and / or the number of ions. Therefore, a mass spectrometer has an ion source, an analyzer, and a detector. All further details are largely dependent on the purpose of the mass spectrometric experiment.

There are a number of different possible GC/MS configurations, but all share similar components. There must be some way of getting the sample into the chromatograph, such as using an injector. This may or may not include sample purification or preparation components. There must be a gas chromatograph, with its carrier gas source and control valve, its temperature control oven, and tubing to connect the injector to the column and out to the mass spectrometer interface. There must be a column packed with support and coated with a stationary phase in which the separation occurs. There must be

an interface module in which the separated compounds are transferred to the mass spectrometer system, made up of the ionization source, focusing lens, mass analyzer, detector, and multistage pumping. Finally there must be a data/control system to provide mass selection, lens and detector control, and date processing (see Figure 2.5).
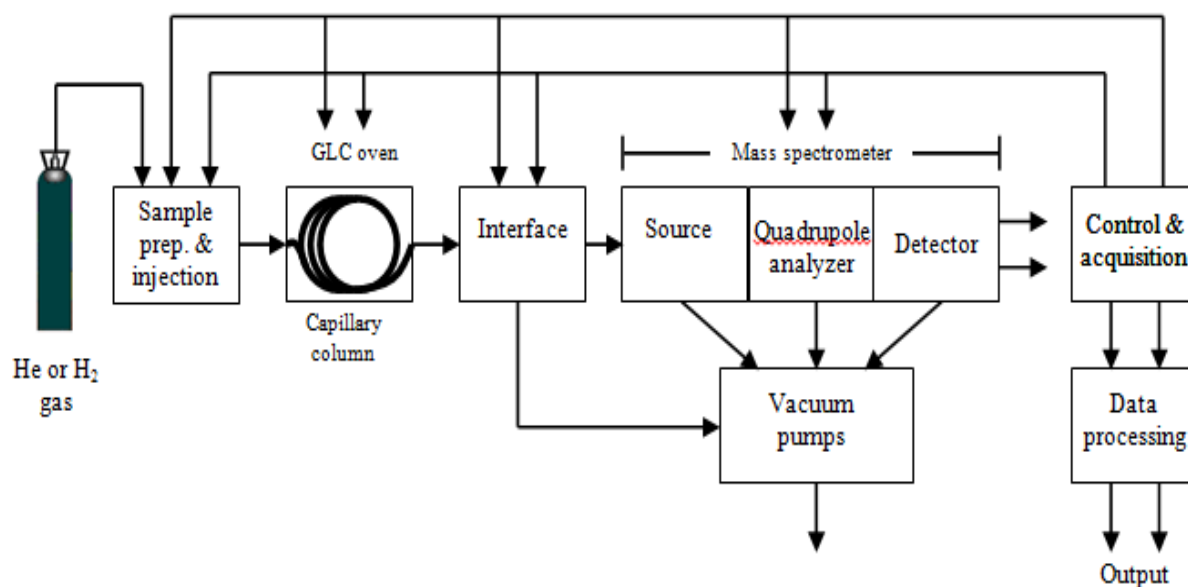
Figure 2.5 Schematic diagram of mass spectrometer system (Bridgwater, 2002)

The injection is a septum port on top of the gas chromatograph through which a sample is injected using a graduated capillary syringe. In some cases, this injection port is equipped with a trigger that can start the oven temperature ramping program and/or send a signal to data/control system to begin acquiring data. For more complex or routine analysis, the injection can be made from an auto-sampler, allowing multiple vial injections an automated chromatography and data processing. For crude samples that need pro-injection processing there are split/splitless injectors, throat liners with different surface geometry, purge and trap systems, head space analyzers, and cartridge purification systems. All provide sample extraction, cleanup, or volatilization prior to the sample being introduced into the gas chromatographic column.

The interface may serve only as a transfer line to carry the pressurized GC output into the evacuated ion source of the mass spectrometer. It can also serve as a sample concentrator by eliminating much of the carrier gas. It can permit carrier gas displacement by a second gas that is more compatible with the desired analysis, that is, carbon dioxide for chemically induced (CI) ionization for molecular weight analysis. It can be used to split

the GC output into separate streams that can be sent to different detectors for simultaneous analysis by completely different methods.

In the evacuated ionization chamber, the sample is bombarded with electrons or charged molecules to produce ionized sample molecules. These are swept into the high-vacuum analyzer where they are focused electrically and then selected in the quadrupole. The electrically charged poles of the quadrupole create a standing magnetic field in which the ions are aligned. Individual masses are selected from this field by sweeping it with a radio frequency signal. As different frequencies are reached, different mass-charge ratio (m/z) ions are able to escape the analyzer and reach the detector. By sweeping from higher to lower frequency, the available range of m/z ions are released one at time to the detector, producing a spectrum.On entering the detector, the ions are deflected into a cascade plate where the signal is multiplied and then sent to the data system as an ion current versus m/z versus time. The summed raw signal can be plotted against time as a total-ion chromatogram (TIC) or a single ion m/z can be extracted and plotted against time as a single-ion fragment can be extracted and plotted over an m/z range producing a mass spectrum. It is important always to remember that the data block produced is three dimensional: m/z versus signal strength versus time. In most other detector the output is simply single strength versus time.

CHAPTER 3

METHODOLOGY

This chapter presents the experimental equipment and procedure used in this study: the preparation of the model bio-oil, which will be used instead of the real pyrolysis bio-oil for test with catalysts; bio-oil upgrading experiments; are analysis of products, especially methods of bio-oil characterization.

3.1 Bio-Oil Preparations

A model bio-oil in this study refers to a mixture of high purity grade chemicals, which were prepared before each experiment and the mixture was used instead of the bio-oil for the preliminary test with the catalysts. Each type of chemicals and their mixing proportions are considered from the main components reported for bio-oil derived from eucalyptus bark (Yuenyongchaiwat, 2010). Typically, pyrolysis bio-oil are consisted of moisture in the range of 15-25 wt% and the chosen moisture proportion in this study is 20 wt%. In this study, model bio-oil will be mixed with no water and 20 wt% of moisture to see the moisture effect on catalytic deoxygenation. The mixtures of model bio-oil in this study are acetone, phenol, furfural, ethanol, acetic acid and de-ionized water with the mixing proportion as shown in Table 3.1.

Table 3.1 The mixing chemicals and proportions in model bio-oil

Chemicals	Mixing Proportions (wt %)	
	no moisture	20% moisture
Acetone	34	27
Phenol	33	26
Furfural	14	12
Ethanol	12	9
Acetic acid	7	6
De-ionized water	-	20
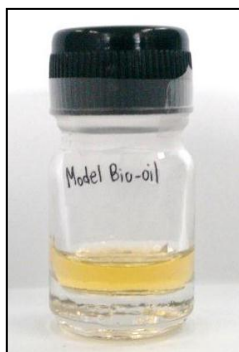
Figure 3.1 The physical appearance of model bio-oil

3.2 Bio-Oil Upgrading Experiments

The bio-oil upgrading experiments were conducted using a mechanically stirred stainless steel autoclave (Amar Model), as shown in Figure 3.2. The reactor volume is 100 ml and operates on a batch mode with a maximum pressure and temperature of 100 bar and 350°C, respectively. The hydrodeoxygenation (HDO) catalysts used in the upgrading experiment were CoMo/Al$_2$O$_3$and NiMo/Al$_2$O$_3$. About 1-5%wt (0.25-1.25g) of each catalyst was loaded in the reactor with 25 g of bio-oil. After closed, the reactor was flushed with nitrogen gas 3 times and pressurized with 3-15 bar initial pressure of hydrogen. The reactor was heated to achieve 250 - 350°C.The reaction time was 3 hours, after which the liquid product was collected for elemental analysis, Karl's Fisher titration and GC/MS, while the gas product was collected for GC analysis. Furthermore, the effect of the stirring rate on mass transfer limitation was checked by varying the stirring rate from 500-1000 rpm.

Figure 3.2 Mechanically stirred stainless steel autoclave**.**

3.3 Bio-Oil Analysis

3.3.1 Elemental Analysis

An elemental Analyzer (Perkin Elmer PE2400 Series II) was used to determine the C, H, S and N contents. The oxygen content was determined by the difference.

3.3.2 Performance of Catalytic Hydrodeoxygenation, %HDO

The performance of catalytic hydrodeoxygenation or %HDO was the percentage of oxygen removal from bio-oil, which can be calculated by the equation below:

$$\%HDO = \left[1 - \frac{\text{Amout of Oxygen in bio-oil after upgrading}}{\text{Amout of Oxygen in bio-oil before upgrading}} \right] \times 100$$

3.3.3 Water Content

The water content in the samples was determined by a Karl Fischer titration using a Metrohm 836 titrando device. The titrations were carried out using the Karl Fischer titrant Hydranal-Composite 5 (Karl Fischer, Fluka). All measurements were performed in duplication.

3.3.4 Gas Chromatography Mass Spectrometry, GC/MS

The compounds in the liquid product were determined by a gas chromatography (Perkin-Elmer, Clarus 500) coupled with a quadrupole mass spectrometer (Perkin-Elmer, Clarus 500 MS), using the separation made on a 29.3×0.25 mm i.d. fused HP-5MS column. The GC oven temperature was held at 50°C for 2 min, and then programmed to 100°C at 10°Cmin^{-1}. Finally, the GC oven temperature was ramped to 280°C at 10°Cmin^{-1} for 10 min, so the total run time was 40 min. The injector temperature was 290°C with split mode 1:40. A 1.0 ml/min of helium was used as the carrier gas.

3.3.5 Gross Calorific Value of bio-oil

Gross calorific value was determined in a calorimetric bomb (ASTM D-4809).

3.4 The Calculation of % Product Distribution

The calculations of the yield of each phase of product from catalytic hydrodeoxygenation experiments are shown as the following equations:

- **The Calculation of Liquid Phase Product**

$$\% \text{ yield of liquid product } (\%W_{aq}) = \frac{W_{aq}}{W_o} \times 100 \qquad (1)$$

$$\% \text{ yield of water in liquid product } (\%W_m) = \frac{\%H_2O}{100} \times \%W_{aq} \qquad (2)$$

$$\% \text{ yield of upgraded oil } (\%W_u) = \%W_{aq} - \%W_m \qquad (3)$$

- **The Calculation of Solid Phase Product**

$$\% \text{ yield of solid product } (\%W_s) = \frac{W_s - W_c}{W_o} \times 100 \qquad (4)$$

- **The Calculation of Gas Phase Product**

$$\% \text{ yield of gas product } (\%W_g) = 100 - \%W_{aq} - \%W_s \qquad (5)$$

Note: W_o is the bio-oil weight input in reactor

W_{aq} is the weight of liquid product, including upgraded oil and moisture

$\%H_2O$ is the moisture in liquid product analyzed by KF titration

W_u is the upgraded oil in liquid product

W_s is the solid product

W_c is the catalyst weight input in reactor

3.5 Gas Analysis

Gas chromatography with a thermal conductivity detector (Shimadzu, GC-14B), as show in Figure 3.3, was used to analyze the CO and CO2 produced from the bio-oil upgrading experiment. Helium was used as the carrier gas with flow of 50 ml/min. The temperature of the porapak Q and molecular sieve column were controlled in the following conditions. The inject line was kept at 60 °C. The oven initial temperature was 60 °C and held for 10 min then programmed to increase to 120 °C at 5 °C/min and held at that temperature for 10 min. For H_2 and hydrocarbon gases product, gas chromatography with a thermal conductivity detector and flame ionization detector (Shimadzu, GC-2014) as shown in Figure 3.4 was used with N_2 carrier gas with flow of 10 ml/min. The temperature of the porapak Q column was controlled with the following conditions. The inject line was kept at 60 °C. The oven initial temperature was 60 °C and held for 10 min then programmed to increase to 180 °C at 20 °C/min and held at that temperature for 10 min. The total volume of gas product was also directly measured by using gas syringe and used to calculate all the detectable gas species in molar basis.

Figure 3.3 Gas Chromatography (Shimadzu, GC-14B)

Figure 3.4 Gas Chromatography (Shimadzu, GC-2014)

3.6 The Experimental Repeatability

For the accuracy of experimental results, the experiment was repeated at 300 °C, 5 bar with NiMo/Al$_2$O$_3$ catalyst. Table 3.2 shows the chemical analysis of the repeated experiments. It was found that the % HDO of those are similar with a standard deviation of 0.29.

Table 3.2 The chemical analysis of experimental repeatability

Catalyst %(w/w)	Temperature (°C)	H$_2$ initial pressure (bar)	Stirring velocity (rpm)	Elemental Analysis			%HDO	SD
				C	H	O		
5	300	5	750	70.71	7.43	21.86	30.27	0.29
5	300	5	750	70.88	7.37	21.75	30.62	

CHAPTER 4

RESULTS AND DISCUSSION

This chapter presents the results of the catalytic hydrodeoxygenation of the model bio-oil by using various catalysts. Investigated parameters include stirring rate, temperature, the presence of water and catalyst type and loading.

4.1 The Effect of the Stirring Rate on Mass Transfer Limitation

The effect of the stirring rate on mass transfer limitations was first checked by varying the stirring rate in the range of 500-1000 rpm under otherwise similar conditions. The calculation of product distribution is shown in section 3.5. The results of the product distribution at different stirring rates are shown in Figure 4.1. At 500 rpm, there was a presence of solid products, but these disappeared at higher stirring rates. Increasing the stirring rate above 500 rpm also significantly increased the upgraded oil. However, the stirring rate had much less effect on the yield at the stirring rate above 750 rpm. This suggests that using the stirring rate at a minimum of 1000 rpm can ensure minimized mass transfer limitation.
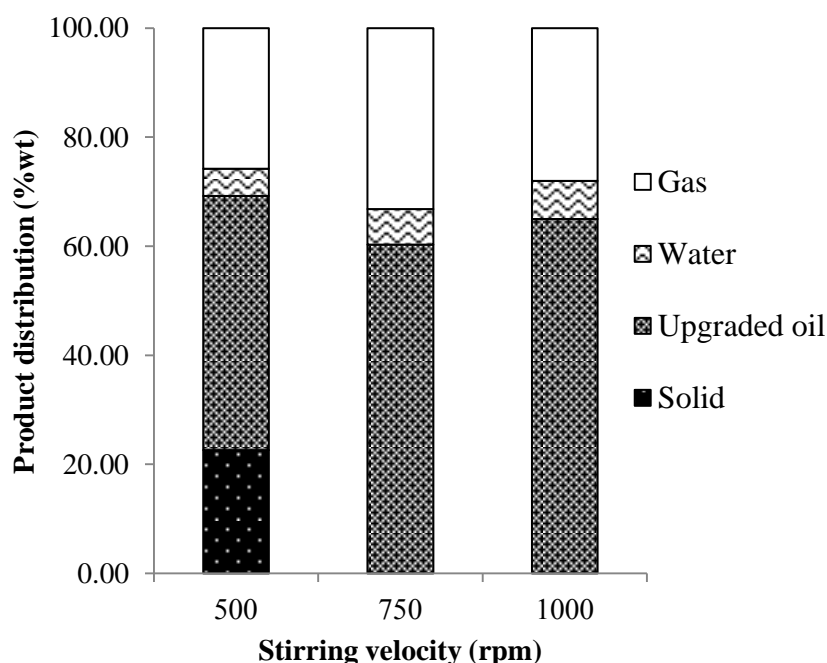
Figure 4.1 The effect of stirring rates on product distribution.

(at 1%wt of CoMo/Al$_2$O$_3$ catalyst, 325°C, 3 bar initial pressure of H$_2$ and 3 hours)

4.2 Bio-Oil Upgrading Using CoMo/Al$_2$O$_3$

    4.2.1 The Effect of Temperature on Catalytic Hydrodeoxygenation Using CoMo/Al$_2$O$_3$

        To study the effects of temperature on the activity of the catalytic hydrodeoxygenation and the composition of gas products, the experiments were conducted at 250-350°C using 1%wt of CoMo/Al$_2$O$_3$, 3 bar of H$_2$ initial pressure and 3 hours of reaction time. The physical appearance of the bio-oil products and the product distribution from the experiment at various operating temperatures were given in Figures 4.2 and 4.3, respectively. The liquid product after reaction consisted of upgraded oil and water from the deoxygenation reaction. It can be observed that solid products started to form when the operating temperature reached 300°C. At higher temperatures, the amount of the solids clearly increased, suggesting the occurrence of heat induced polymerization reactions (Fisk et al., 2009). The amount of gas product also increased with increasing temperature. For the performance of catalytic hydrodeoxygenation or %HDO, %HDO of the bio-oil products are given in Figure 4.3(b). The results clearly show that under the conditions of the study, oxygen removal could be achieved and was favored by the increase in temperature. The %HDO increased from around 24.34 to 28.36% when the temperature increased from 300 to 325°C. It was found that operating at 350°C completely destroyed the catalyst activity due to thermally induced polymerization and the formation of coke (Samolada et al., 1998; Furimsky, 2000; Furimsk et al., 1999). Thus, the maximum temperature was limited to be 325°C for all experiments.
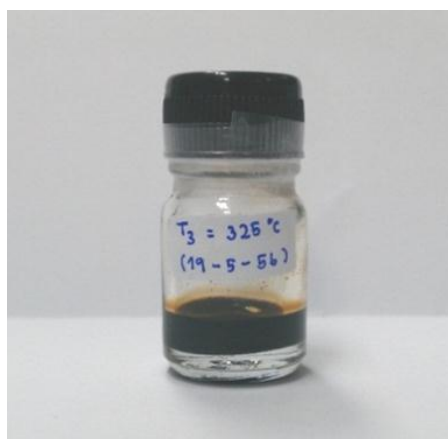
Figure 4.2 The upgraded bio-oil products
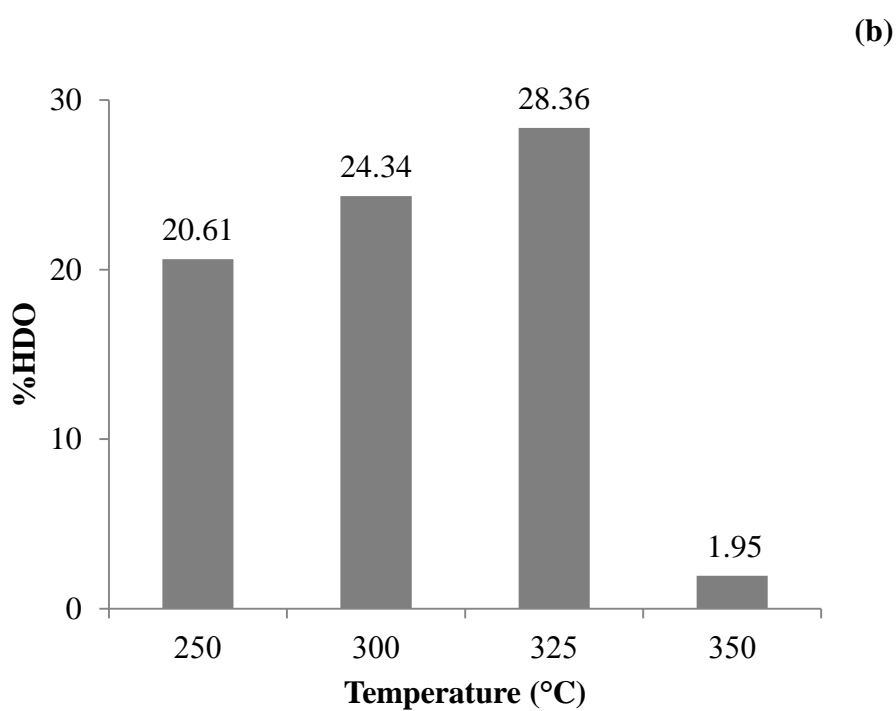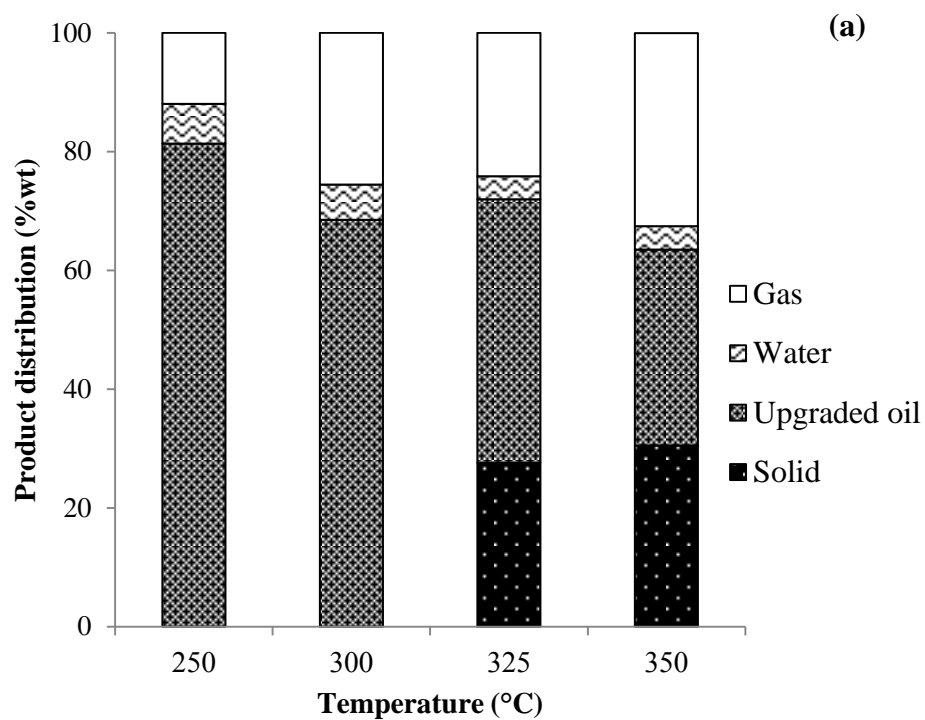
Figure 4.3 The effect of operating temperature of catalytic hydrodeoxygenation using CoMo/Al$_2$O$_3$on (a) product distribution and (b) %HDO (at 1%wt of CoMo/Al$_2$O$_3$ catalyst with 1-2 mm of particle size, 3 bar initial pressure of H$_2$ and 3 hours)

In order to explain the mechanism behind the HDO reaction, the H_2 consumption and the amount of the major product gas species were determined by the GC analysis and the direct measurement of the total product gas volume. The calculation of product gases is shown in Appendix A and the results are shown in Figure 4.4 as a function of operating temperatures.
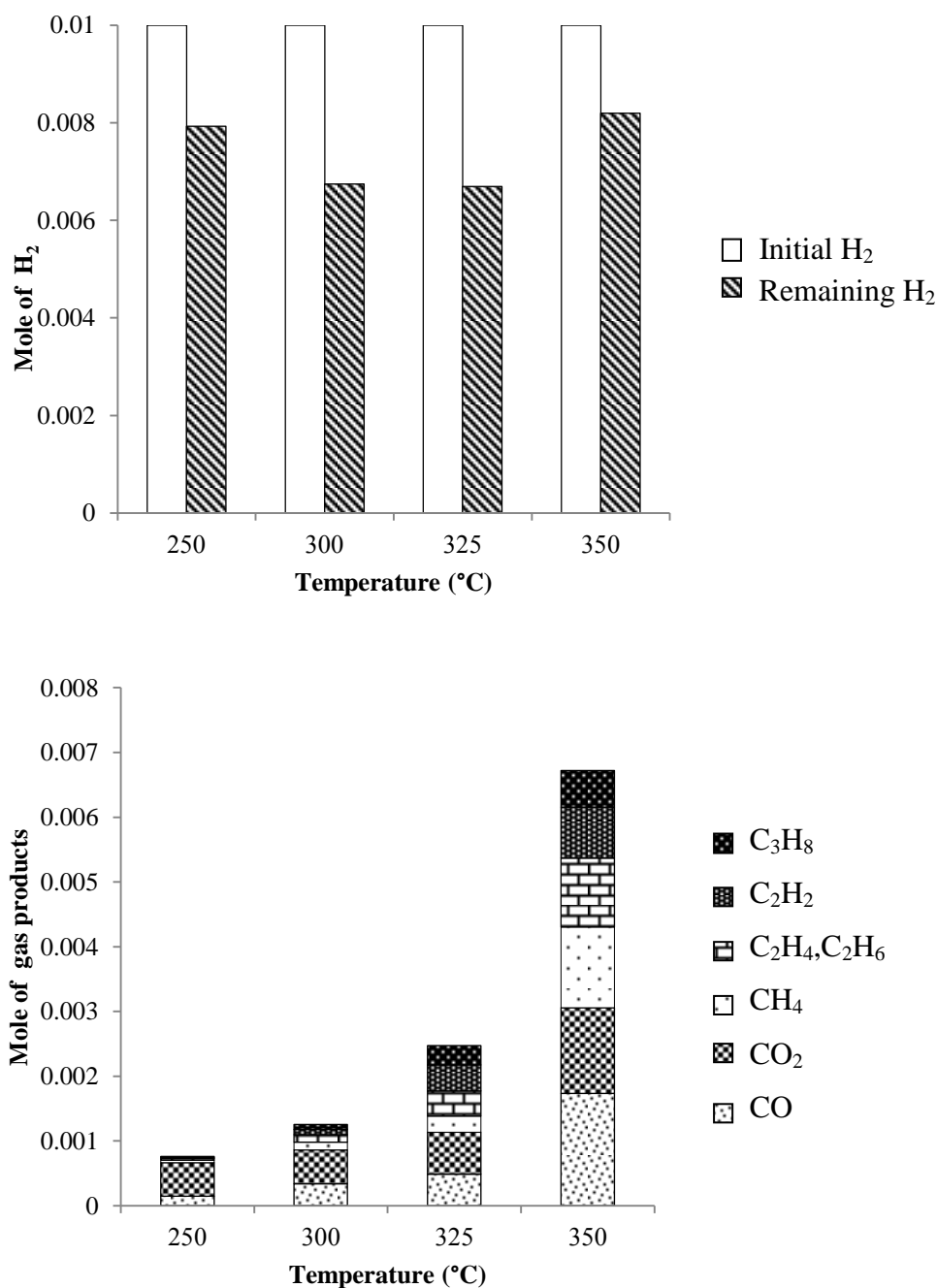
Figure 4.4 The effect of operating temperature of catalytic hydrodeoxygenation using $CoMo/Al_2O_3$ on the composition of gas products.

H_2, CO, CO_2, CH_4, C_2H_2, C_2H_4, C_2H_6 and C_3H_8 were the gas products detected. Provided with the same initial amount of H_2, the remaining H_2 decreased with increasing temperature, except at 350°C when the catalyst activity was completely destroyed, as explained earlier. The decreased H_2 in the product gas suggests that the H_2 consumption was promoted by temperature according to the hydrodeoxygenation reaction (1) (Mortensen, 2013):

Hydrodeoxygenation reaction $\quad\quad$ R-OH + $H_2 \rightarrow$ R-H +H_2O $\quad\quad\quad$ (1)
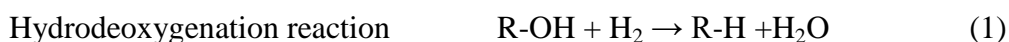
This result was also confirmed by the increased production of all hydrocarbon gas species. In addition, CO and CO_2 were produced. Shabaker et al. (2004) reported that higher reaction temperatures caused the cracking of the macromolecules in the oil fraction, resulting in higher amounts of gas products. CO and CO_2 are likely to form by the carbonylation reaction (2) and carboxylation reaction (3) (Bakhshi, 1995; Wildschut, 2009).

Decarbonylation reaction $\quad\quad\quad$ R_1-COH $\rightarrow R_1$-H + CO $\quad\quad\quad$ (2)

Decarboxylation reaction $\quad\quad\quad$ R_1-COOH $\rightarrow R_1$-H + CO_2 $\quad\quad$ (3)
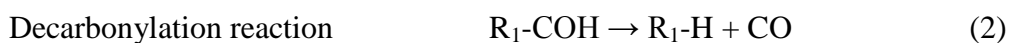
4.2.2 The Effect of the Presence of Water in Bio-Oil on Catalytic Hydrodeoxygenation Using CoMo/Al$_2$O$_3$

From the hydrodeoxygenation data of bio-oil without water mentioned in Section 4.2.1, the operating temperature at 325 °C showed the highest hydrodeoxygenation performance; therefore, this condition was selected to test the effect of the presence of 20 wt% of water in bio-oil. With the presence of water in bio-oil (see Figure 4.5), the formation of solid was similarly found but the %HDO was considerably reduced from 28.36% to 7.73% due to the water inhibition to the hydrodeoxygenation activity of catalyst (Senol, 2007). However, the water produced from the reaction, which was determined by subtracting the water originally present before upgrading from the total water after the upgrading, was not different.
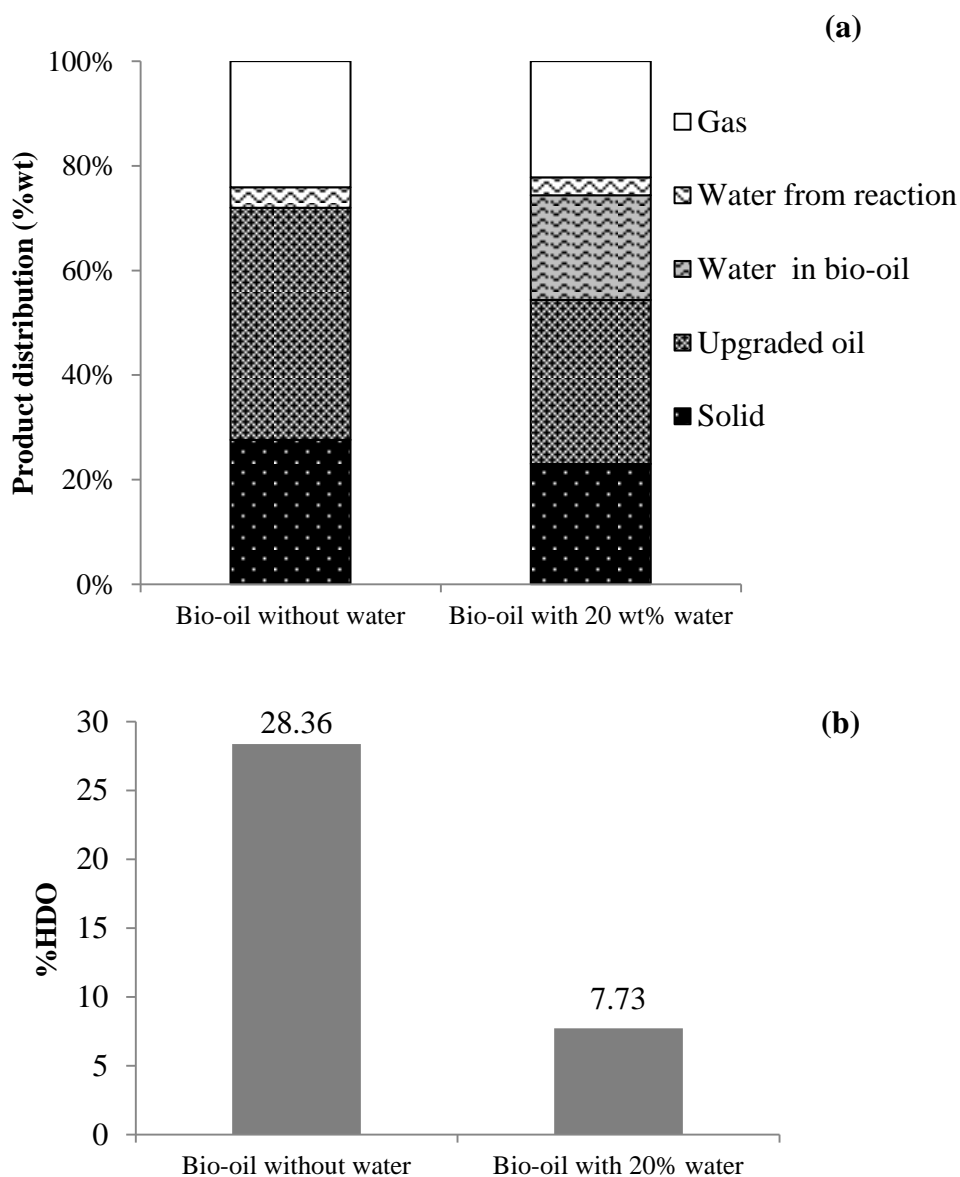
Figure 4.5 The effect of the presence of water in bio-oil on (a) product distribution and (b)%HDO (at 1%wt of CoMo/Al$_2$O$_3$ catalyst with 1-2 mm of particle size, 325°C, 3 bar initial pressure of H$_2$ and 3 hours).

The activity of the catalyst to reduce oxygen in oil decreased as a result of the water added in the oil. The use of hydrogen in the reaction and the yield of gas products also decreased as seen in Figure 4.6. However, CO$_2$ appears to increase due to the promotion of water (in bio-oil) on CO consumption via water gas shift reaction (4), a moderately exothermic reversible reaction (Choi et al., 2003):

Water gas shift reaction $\qquad$ $CO+H_2O \leftrightarrow CO_2+H_2$ $\qquad$ (4)
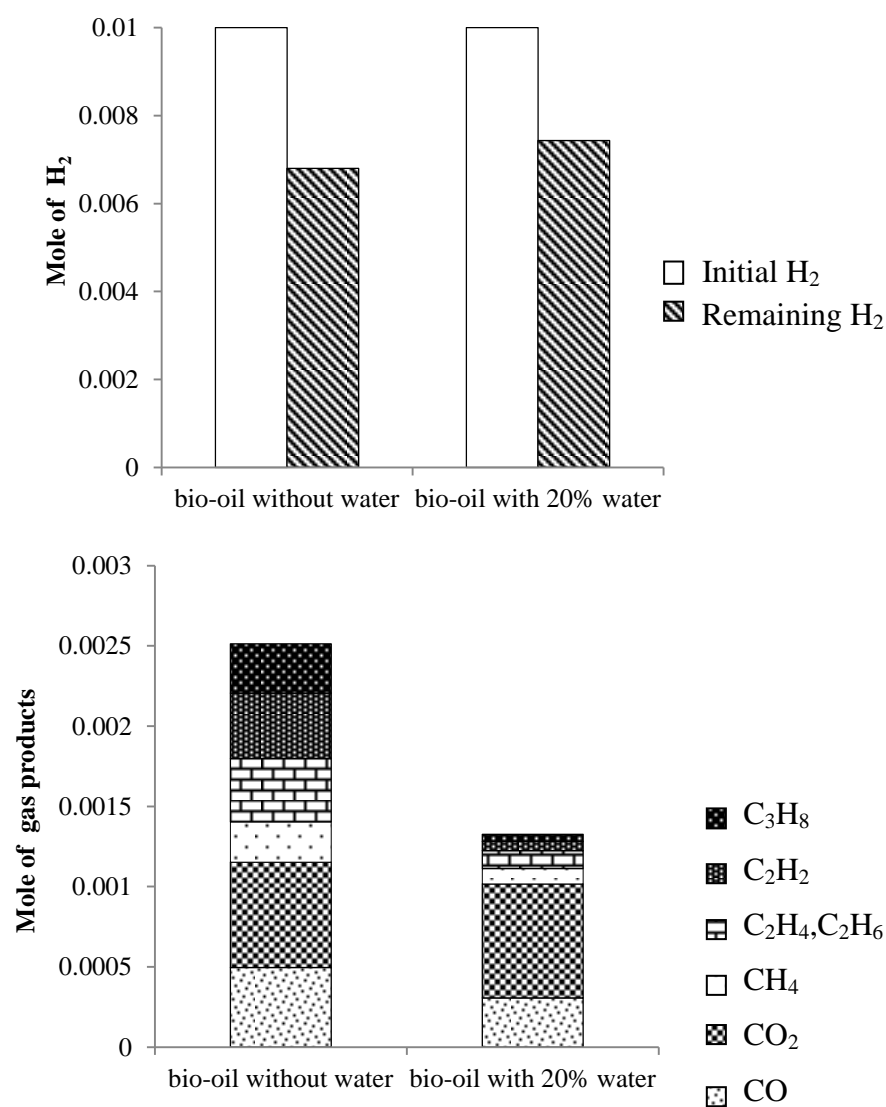
Figure 4.6 The effect of the presence of water in bio-oil on the composition of gas products.

4.2.3 The Effect of the %wt of Catalyst on Catalytic Hydrodeoxygenation Using CoMo/Al₂O₃

The effect of %wt of catalyst on catalytic hydrodeoxygenation was determined by comparison between using 1%wt and 5 %wt of $CoMo/Al_2O_3$ at 325 °C for 3 hours. The results in Figure 4.7(b) indicated that % HDO was increased in the presence of catalyst and even more at higher dosage. Increasing catalyst from 1%wt and 5 %wt resulted in the increase of %HDO from 18.90% to 20.93%.
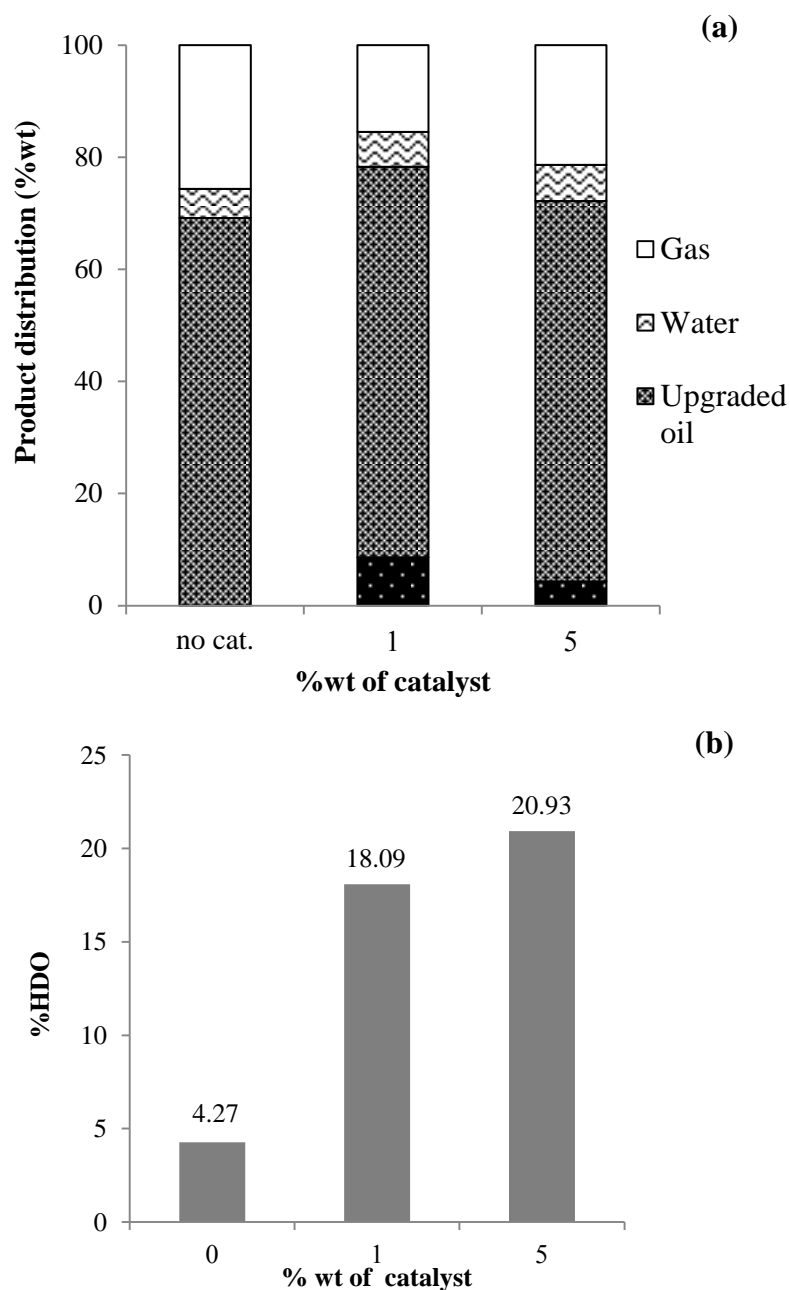
Figure 4.7 The effect of %wt of $CoMo/Al_2O_3$ catalyst on (a) product distribution and (b) %HDO (at 325°C, 0.5-1.0 mm of $CoMo/Al_2O_3$ catalyst size, 5 bar initial pressure of H_2 and 3 hours).

The compositions of the gas products are shown in Figure 4.8. These indicate that the increase in catalyst dosing from 1 to 5%wt resulted in increasing of H_2. This additional H_2 present is likely to be the product of the water gas shift reaction which is promoted in the presence of catalyst and is confirmed by the significant decrease in CO.
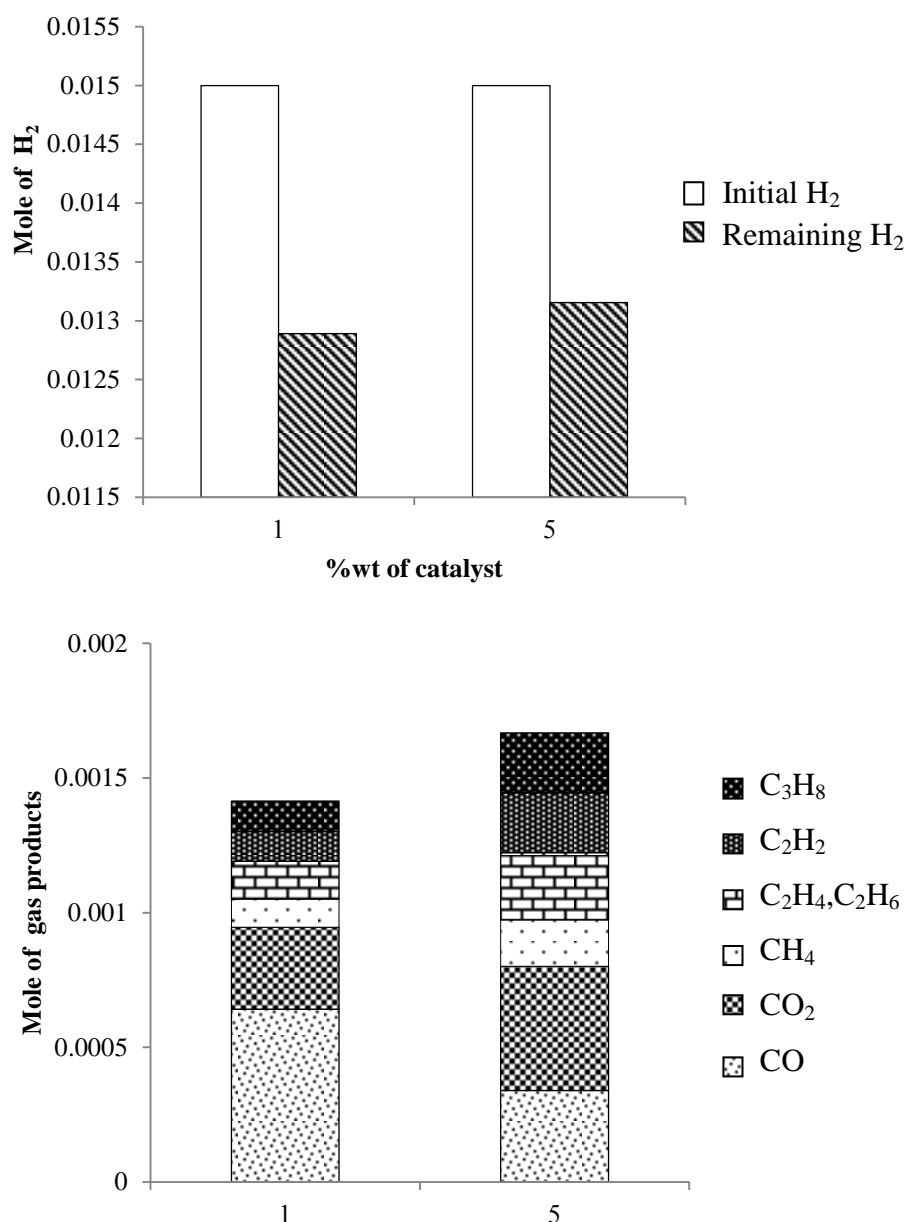
Figure 4.8 The effect of %wt of catalyst on the compositions of gas products.

4.2.4 The Mass Balance of Bio-Oil Upgrading Using CoMo/Al₂O₃

The mass balance of catalytic hydrodeoxygenation of bio-oil without water operated at 325°C, 3 bar initial pressure of H_2 and 3 hours of reaction time is shown in Figure 4.9. The main products of the reaction were in the liquid phase, which is a mixture of upgraded bio-oil and water formed by the reaction, together accounting for 74.3% by mass. The solid and gas products formed are 8.3 and 17.4% by mass, respectively. The carbon balance is shown in Figure 4.10. The majority of carbon is also found in the liquid phase, i.e. about 49.3% by mass, and in the solid phase, 5.8 % by mass.

```
┌─────────────────────────────────────────────────────────────────────────┐
│ Mass balance                    ┌──────────────────────┐                  │
│                                 │ Bio-oil without water│                  │
│ Basis: 100 g of bio-oil feed    │        (100)         │                  │
│                                 └──────────┬───────────┘                  │
│                          ┌─────────────────┴──────────────┐               │
│                          │ Catalytic HDO using CoMo/Al₂O₃  │               │
│                          └─────────────────┬──────────────┘               │
│          ┌───────────────────────┬─────────┴──────┬──────────────────┐    │
│  ┌───────┴────────┐      ┌────────┴───────┐   ┌────┴──────────┐            │
│  │ Solid product  │      │ Liquid product │   │ Gases product │            │
│  │    (8.3)       │      │    (74.3)      │   │    (17.4)      │            │
│  └────────────────┘      └────────┬───────┘   └───────────────┘            │
│                    ┌──────────────┴──────┐                                 │
│            ┌───────┴────────┐     ┌───────┴──────┐                         │
│            │ Upgraded bio-oil│     │    Water     │                         │
│            │    (66.4)      │     │    (7.9)     │                         │
│            └────────────────┘     └──────────────┘                         │
└─────────────────────────────────────────────────────────────────────────┘
```
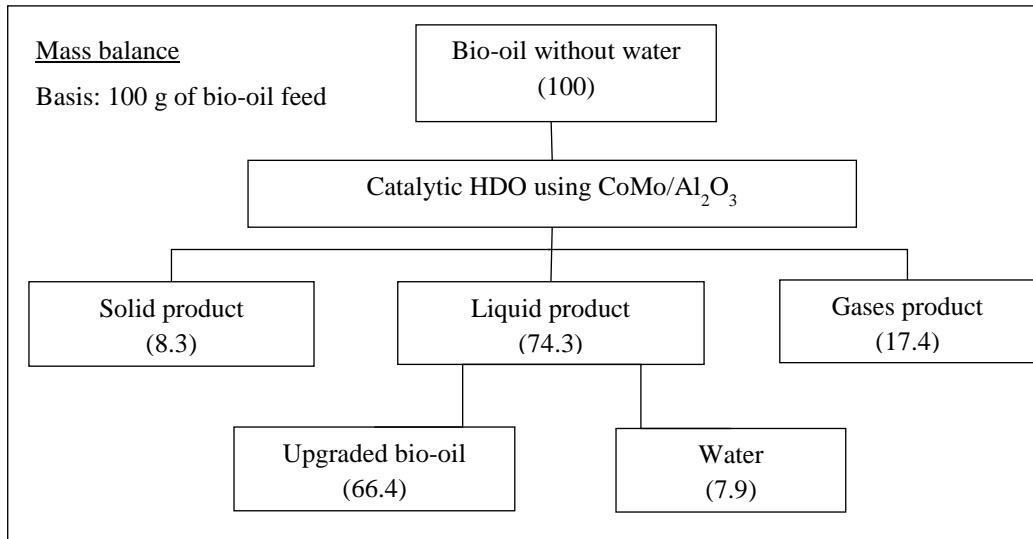
Figure 4.9 The mass balance of catalytic hydrodeoxygenation of bio-oil without water using CoMo/Al$_2$O$_3$.

```
┌─────────────────────────────────────────────────────────────────────────┐
│ Carbon balance                  ┌──────────────────────┐                  │
│                                 │ Bio-oil without water│                  │
│ Basis: 100 g of bio-oil feed    │       (60.7)         │                  │
│                                 └──────────┬───────────┘                  │
│                          ┌─────────────────┴──────────────┐               │
│                          │ Catalytic HDO using CoMo/Al₂O₃  │               │
│                          └─────────────────┬──────────────┘               │
│          ┌───────────────────────┬─────────┴──────┬──────────────────┐    │
│  ┌───────┴────────┐      ┌────────┴───────┐   ┌────┴──────────┐            │
│  │ Solid products │      │ Liquid products│   │ Gas products  │            │
│  │    (5.8)       │      │    (49.3)      │   │    (5.6)       │            │
│  └────────────────┘      └────────┬───────┘   └───────────────┘            │
│                    ┌──────────────┴──────┐                                 │
│            ┌───────┴────────┐     ┌───────┴──────┐                         │
│            │ Upgraded bio-oil│     │    Water     │                         │
│            │    (49.3)      │     │     (-)      │                         │
│            └────────────────┘     └──────────────┘                         │
└─────────────────────────────────────────────────────────────────────────┘
```
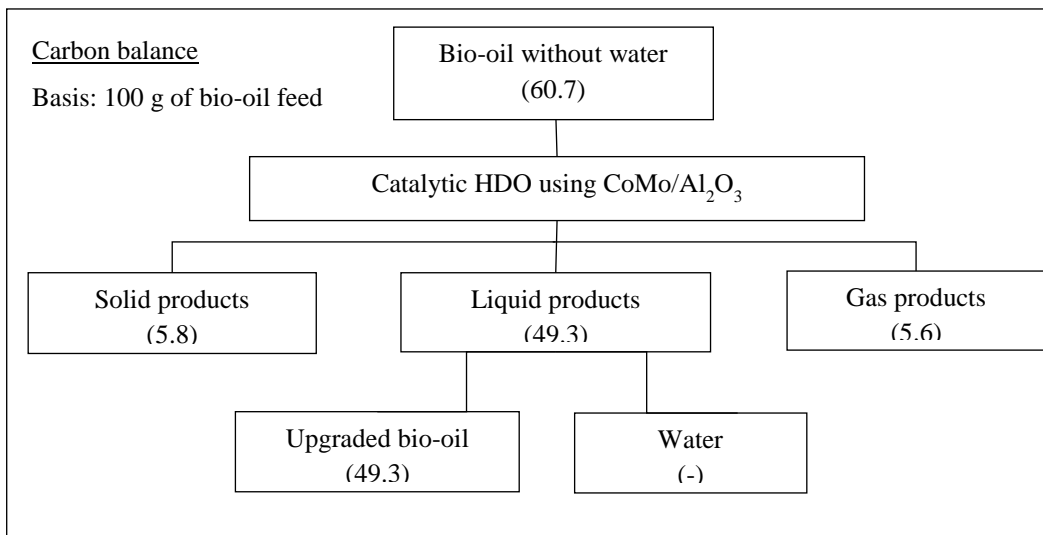
Figure 4.10 The carbon balance of catalytic hydrodeoxygenation of bio-oil without water using CoMo/Al$_2$O$_3$.

The carbon in the gas phase is 5.6 %, which was in the form of CO, CO$_2$ and small molecule of hydrocarbons, such as CH$_4$, C$_2$H$_6$ and C$_3$H$_8$, etc. It can conclude that the improvement of bio-oil quality by catalytic hydrodeoxygenation can give a good result in the removal of oxygen from the bio-oil but this process also causes a loss of carbon from the bio-oil into gas and solid form. Therefore, a followed treatment with a more precise operation condition or a more effective catalysts would be necessary to the fully completion of a high conversion for oxygenated compounds in bio-oil and reduce losses in the form of an unwanted product (solid and gas product).

```
┌─────────────────────────────────────────────────────────────────────────┐
│  Oxygen balance              ┌──────────────────────────┐                 │
│  Basis: 100 g of bio-oil feed│   Bio-oil without water  │                 │
│                              │        (32.0)            │                 │
│                              └──────────────────────────┘                 │
│                   ┌────────────────────────────────────────┐              │
│                   │   Catalytic HDO using CoMo/Al₂O₃        │              │
│                   └────────────────────────────────────────┘              │
│   ┌──────────────┐      ┌──────────────┐      ┌──────────────┐           │
│   │Solid products│      │Liquid products│     │ Gas products │           │
│   │    (-)       │      │    (18.3)    │      │    (13.7)    │           │
│   └──────────────┘      └──────────────┘      └──────────────┘           │
│           ┌──────────────┐      ┌──────────────┐                          │
│           │Upgraded bio-oil│    │    Water     │                          │
│           │    (11.3)    │      │    (7.0)     │                          │
│           └──────────────┘      └──────────────┘                          │
└─────────────────────────────────────────────────────────────────────────┘
```
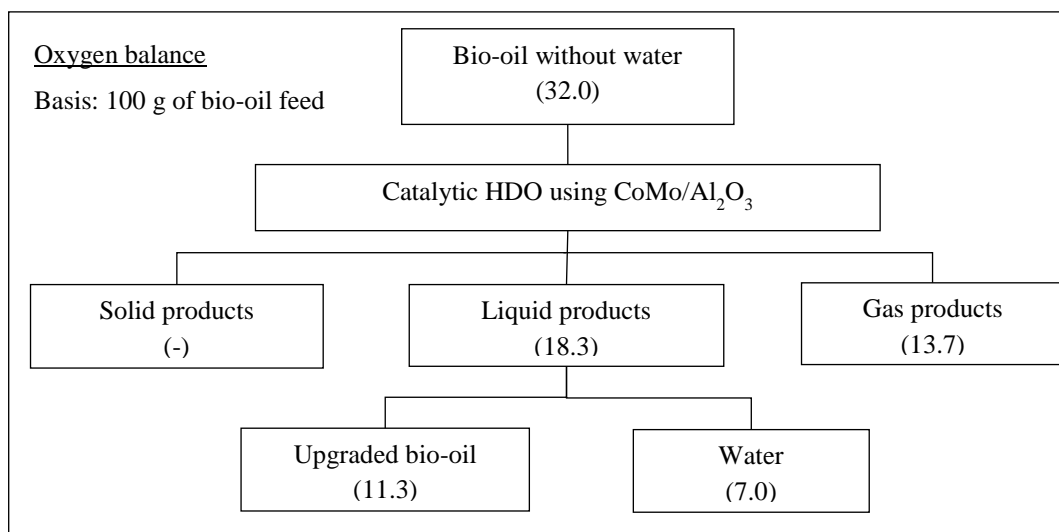
Figure 4.11 The oxygen balance of catalytic hydrodeoxygenation of bio-oil without water using $CoMo/Al_2O_3$

In Figure 4.11, the oxygen balance shows the pathway in which the oxygen was removed from the bio-oil. The oxygen in the bio-oil was mainly eliminated in the form of gas products (CO and CO_2), which were around 13.7 %, and oxygen, which was around 7.0% was removed in the form of water.

4.2.5 The Effect of Operating Condition on Chemical Composition of Upgraded Bio-Oil Using $CoMo/Al_2O_3$

The components of the model bio-oil before the catalytic upgrading were acetone, phenol, furfural, ethanol and acetic acid. The composition in the bio-oil before and after catalytic hydrodeoxygenation was monitored by gas chromatography – mass spectrometry (GC-MS). Figure 4.12 shows the GC/MS chromatogram of detectable compounds after catalytic upgrading. The peaks found included both the compounds in the model bio-oil (i.e. phenol, acetone, ethanol and acetic acid) and the compounds produced from the reaction. Substituted phenol such as 4-Methylphenol, 2-ethyl phenol and 4-ethylphenol and other compounds such as ethyl acetate, 2-methylbenzofuran, naphthalene, etc, were detected. The results suggest that not all compounds in the model bio-oil underwent complete reaction.
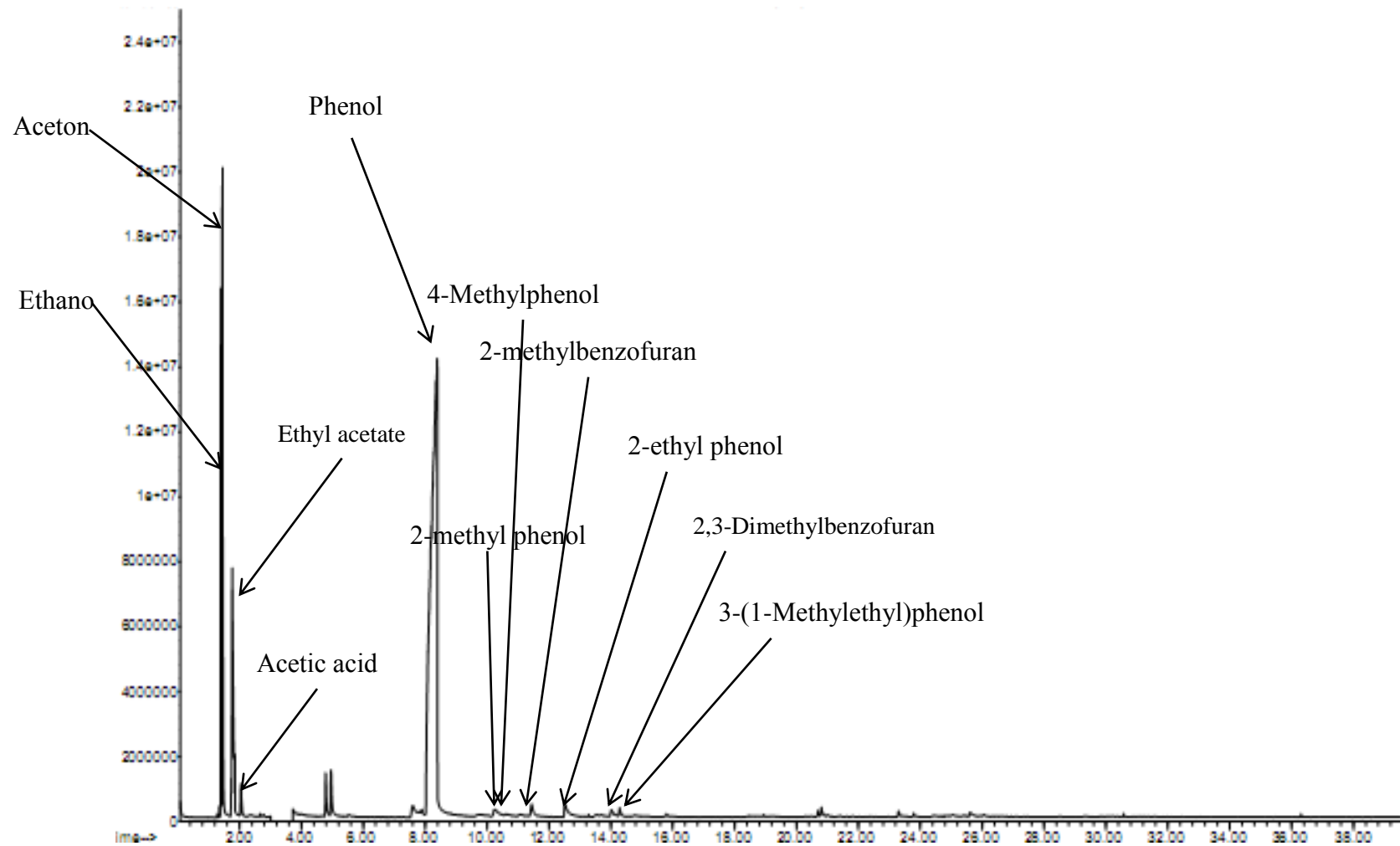
Figure 4.12 GC-MS chromatogram of bio-oil without water after deoxygenation catalyzed by CoMo/Al$_2$O$_3$ at 325°C for 3 hours**.**
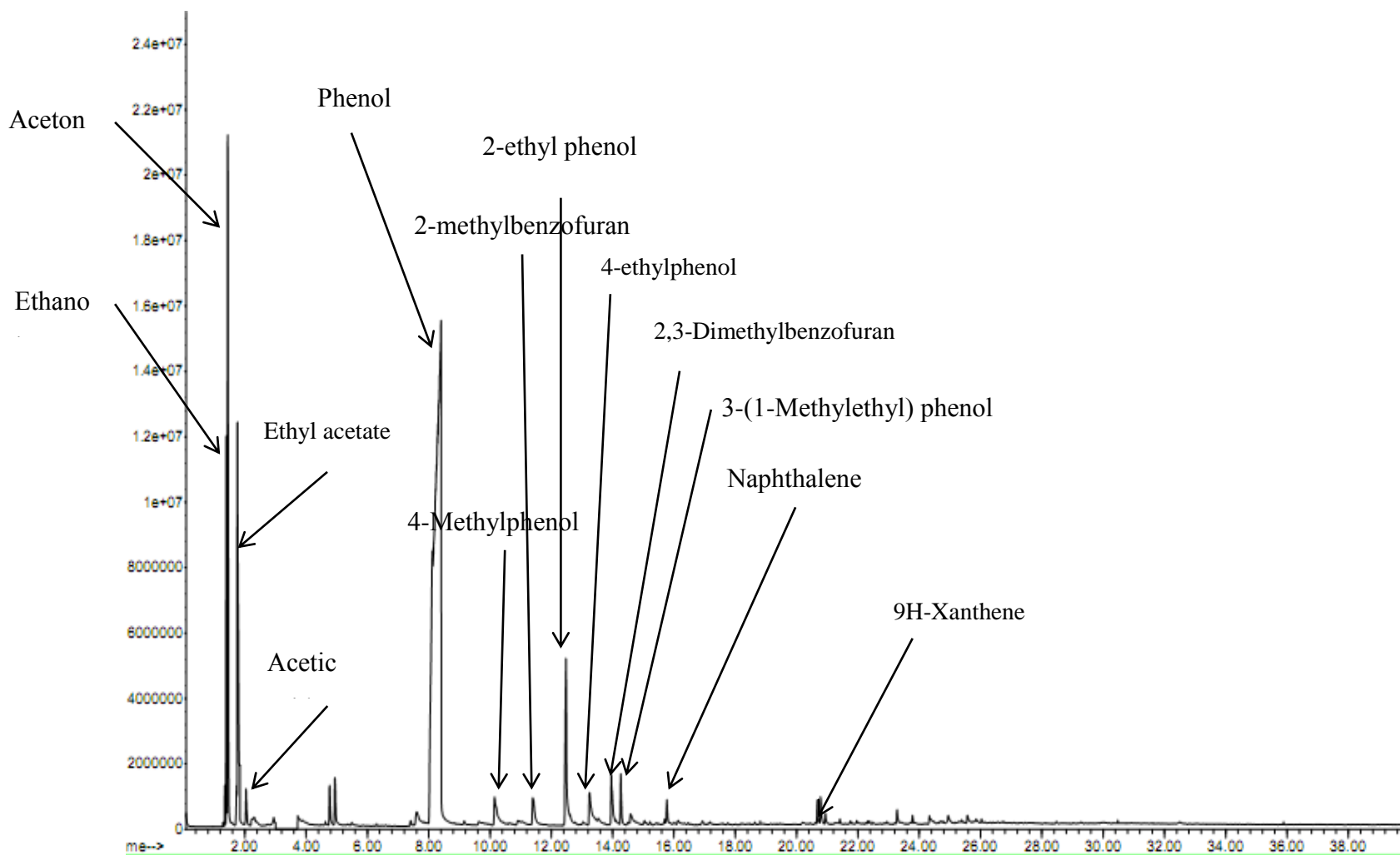
Figure 4.13 GC-MS chromatogram of bio-oil with 20%wt of water after deoxygenation catalyzed by CoMo/Al$_2$O$_3$ at 325°C for 3 hours

According to previous literature (Furimsky, 2000), the researcher studied the effect of H_2 consumption on reactivity of various oxygenated compounds. The highly reactive compounds, like ketones, were easily converted with low H_2 consumption and can be initially deoxygenated at 200°C. However, the complex molecules, like phenols, might suffer the hydrogenation/saturation of the molecules and therefore the complex molecules need more H_2 consumption and higher operating temperature to enhance the degree of oxygen removal.

To consider the presence of water in bio-oil, Figure 4.13 shows the GC-MS chromatogram of bio-oil with 20%wt of water after deoxygenation by using $CoMo/Al_2O_3$ at 325°C for 3 h. Similarly to the case of model bio-oil without water, peaks of original compounds in model bio-oil (i.e. phenol, acetic acid, acetone and ethanol) are higher than those of product compounds. This difference is larger for the case of model bio-oil with water, which implies that the water in bio-oil affected the lower hydrodeoxygenation activity of the catalyst.

4.3 Bio-Oil Upgrading Using NiMo/Al$_2$O$_3$

4.3.1 The Effect of Temperature on Catalytic Hydrodeoxygenation Using NiMo/Al$_2$O$_3$

To study the effects of temperature on the activity of catalytic hydrodeoxygenation and composition of gaseous products, the bio-oil was catalyzed by using 5%wt of $NiMo/Al_2O_3$ for 3 hours. The results in Figure 4.14(b) clearly show that the increase in the reaction temperature from 275-325 °C enhanced the efficiency of the catalyst to remove the oxygenated molecules in bio-oil as 26.03 to 30.85 %, but it can be seen that the solid content increased from ca. 0.21% to 1.05 %wt and gas content increased a little as well. Considering the product yields, it could be seen that the higher reaction temperature increased the contents of solid and gas products while lowering the amount of upgraded bio-oil (see Figure 4.14(a) and Figure 4.15).
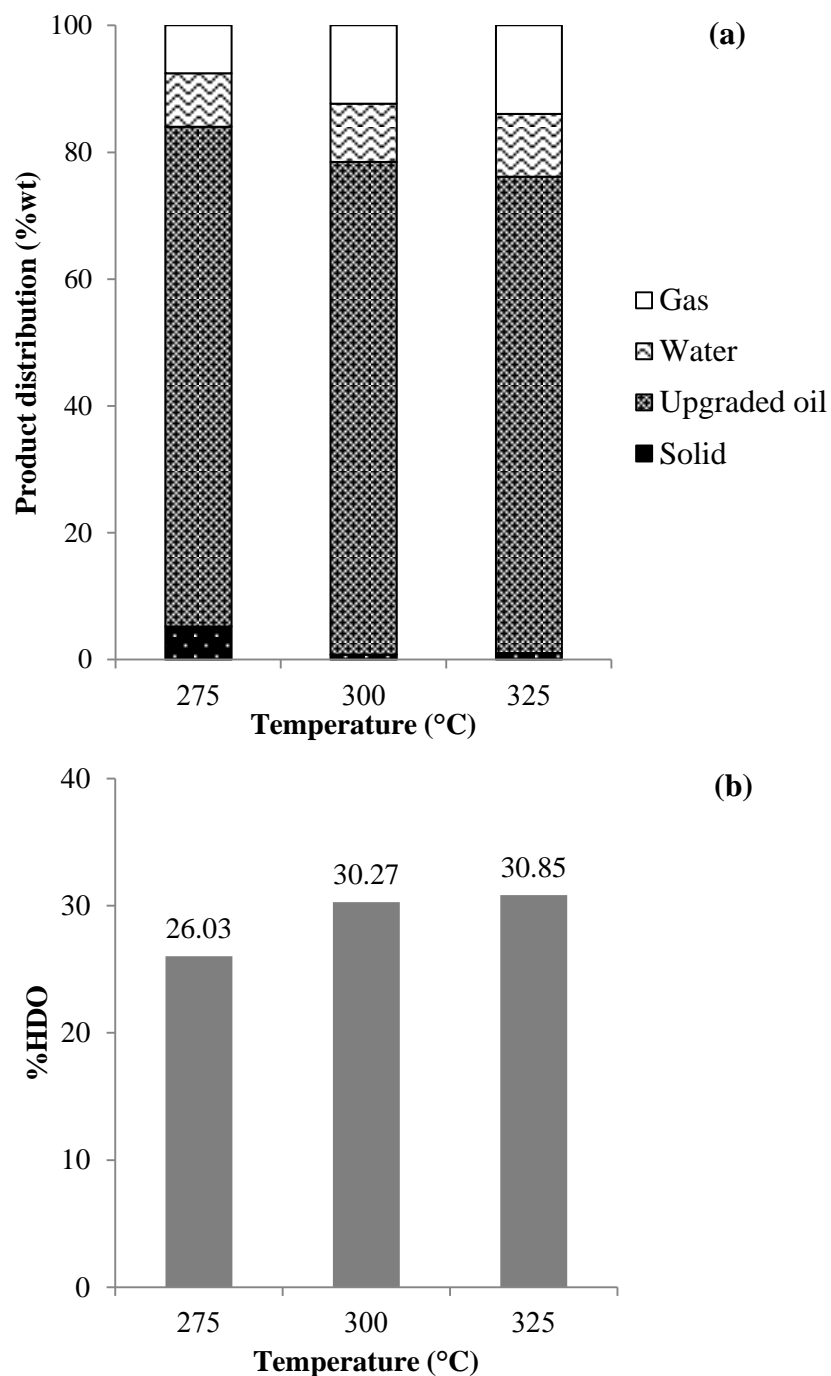
Figure 4.14 The effects of operating temperature of catalytic HDO using NiMo/Al$_2$O$_3$on (a) product distribution and (b) %HDO (at 5%wt of NiMo/Al$_2$O$_3$ catalyst, 5 bar initial pressure of H$_2$ and 3 hours)

The H$_2$ consumption and composition of gas products from different operating temperatures are shown in Figure 4.15. The results showed that the H$_2$ consumption increased continuously as a function of temperature. CO$_2$, CO, CH$_4$, C2H$_2$, C$_2$H$_4$, C$_2$H$_6$ and C$_3$H$_8$ were produced in the upgrading experiment using NiMo/Al$_2$O$_3$ and their content also increased with increasing operating temperature.
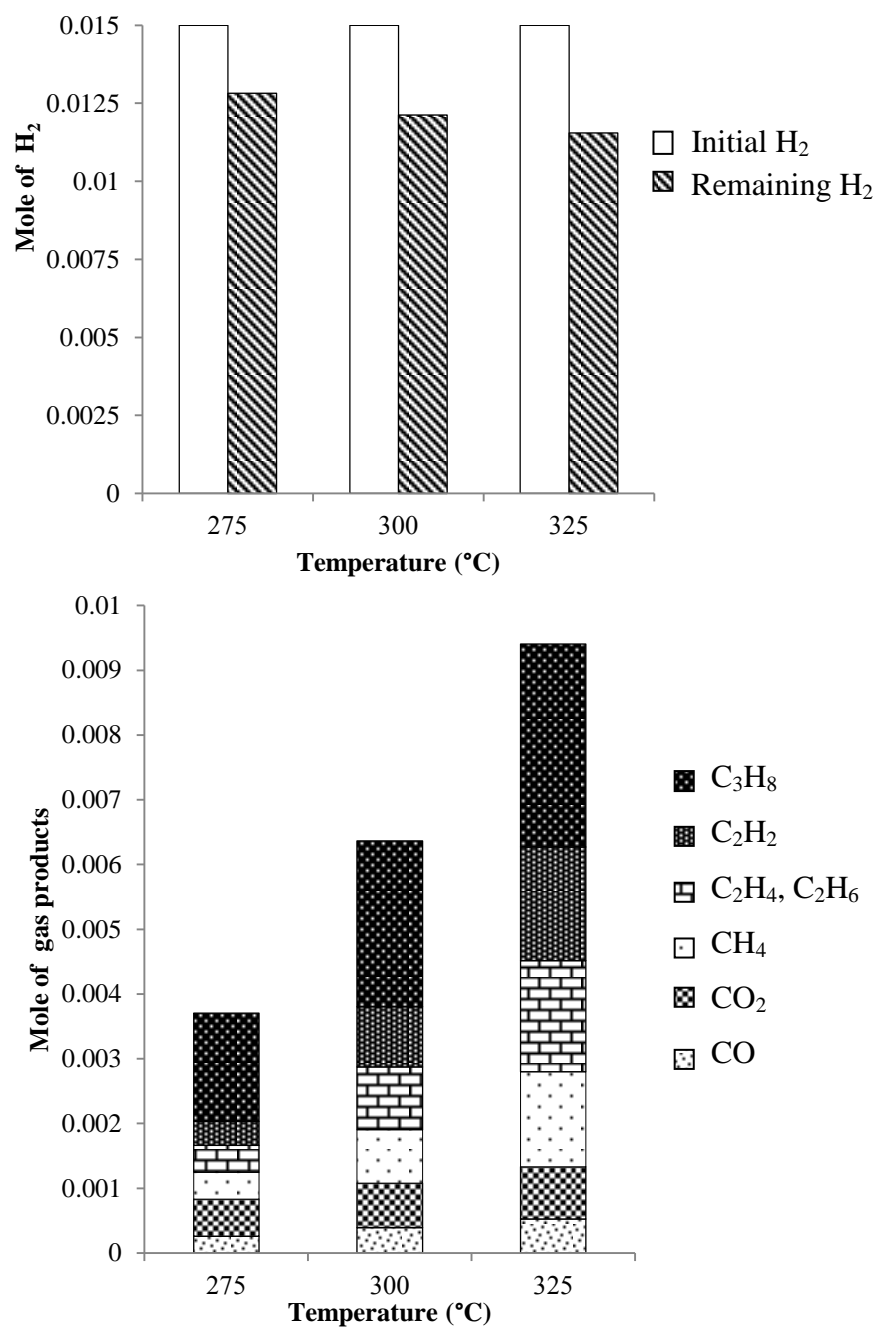
Figure 4.15 The effects of operating temperature of catalytic HDO using NiMo/Al$_2$O$_3$ on the composition of gas products.

4.3.2 The Effect of H$_2$ Initial Pressure on Catalytic Hydrodeoxygenation Using NiMo/Al$_2$O$_3$

The effect of initial pressure of H$_2$ on catalytic hydrodeoxygenation was determined by varying the initial pressure of H$_2$ in the range of 5-15 bar under otherwise

similar conditions. Due to the maximum pressure of the autoclave reactor, the operating temperature was 300°C to keep the final pressure below 100 bar. The product distributions were not significantly different as seen in Figure 4.16(a). The %HDO (see Figure 4.16(b)) also increased from 30.27 to 37.38% when the initial pressure of H_2 increased from 5 to 15 bar. The high pressure has been found to result higher solubility of H_2 in the oil and thereby a higher availability of H_2 in the vicinity of the catalyst. This increases the reaction rate and further decreases coking in the reactor (Venderbosch et al., 2010; Oasmaa et al., 2010; Kwon, 2011).
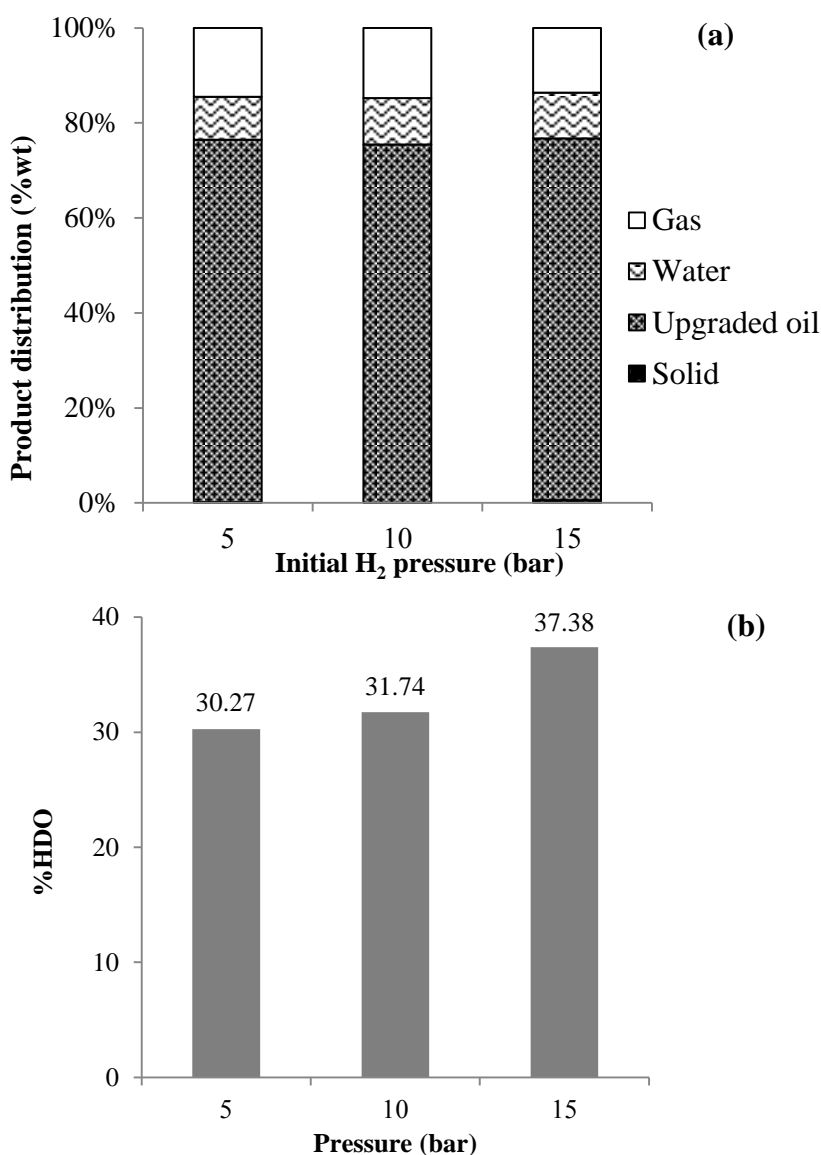
Figure 4.16 The effects of initial pressure of H_2 of catalytic hydrodeoxygenation using NiMo/Al$_2$O$_3$on (a) product distribution and (b) %HDO (at 5%wt of NiMo/Al$_2$O$_3$ catalyst, 300°C and 3 hours)

The compositions of the gas products are presented in Figure 4.17. The H_2 remaining as well as other gas products such as CO, CO_2, CH_4, etc., increased when higher initial pressure of H_2 was used.
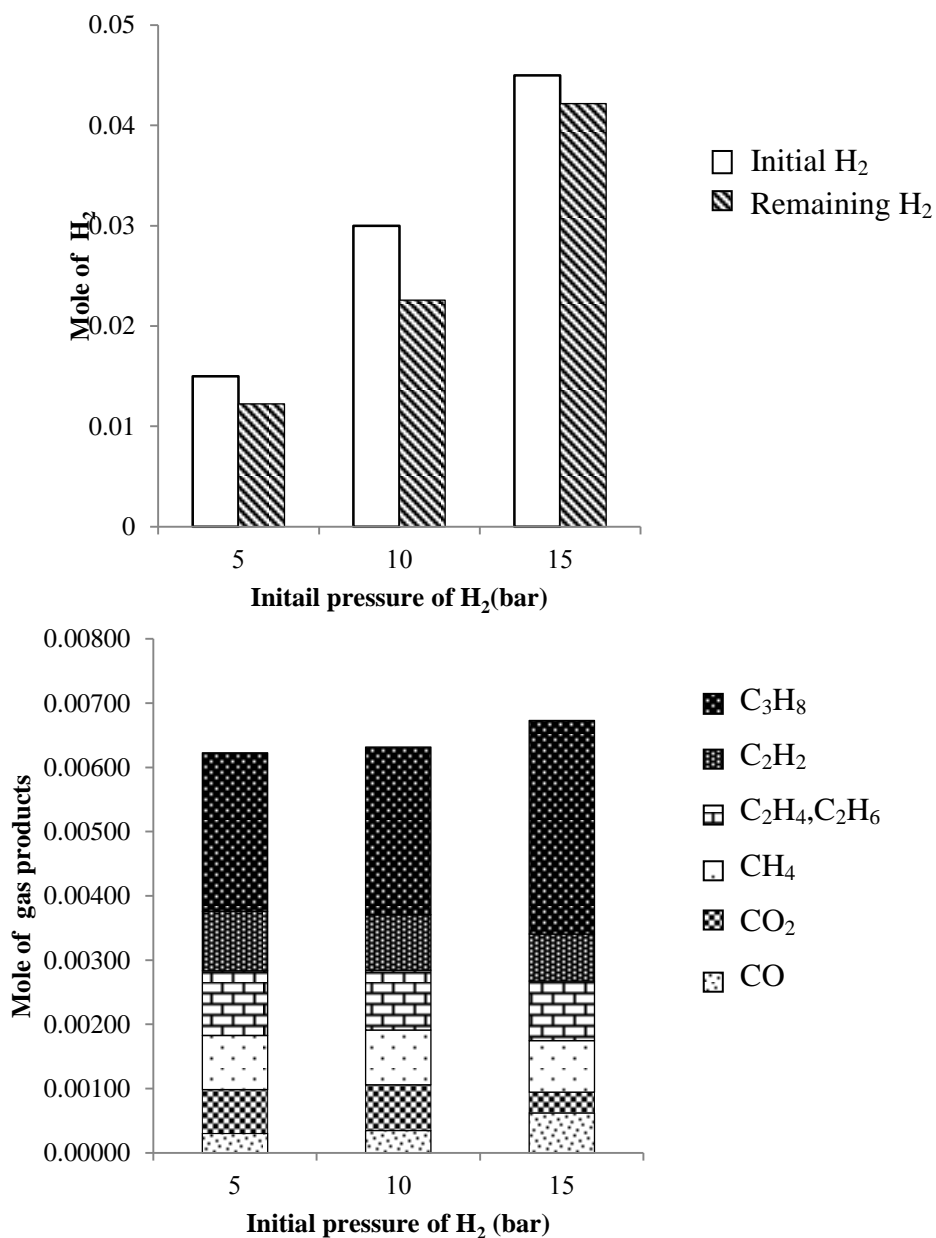
Figure 4.17 The effect of the initial pressure of H_2 of catalytic hydrodeoxygenation using NiMo/Al_2O_3 on the composition of gas products.

4.3.3 The Effect of Reaction Time on Catalytic Hydrodeoxygenation Using NiMo/Al_2O_3

The effect of reaction time on upgraded model bio-oil was considered in this study. The reaction time was varied from 3 to 6 hours under similar conditions, i.e. at 5%wt catalyst, 300°C and 5 bar initial pressure of H_2. The product distribution and percentage of

oxygen removal at various reaction times are presented in Figure 4.18. The product distribution from the experiments showed that longer reaction time slightly increased the contents of solid and gas products while the amount of upgraded bio-oil decreased. For oxygen removal, the results in Figure 4.18(b) indicated that %HDO at 3 and 6 hours were 30.27 % and 32.98%, respectively. This can be explained that with the longer reaction time, catalyst had the longer time to react with oxygen molecules in bio-oil leading to decrease the oxygen content in bio-oil. Thus, increasing reaction time enhanced the efficiency of catalyst.
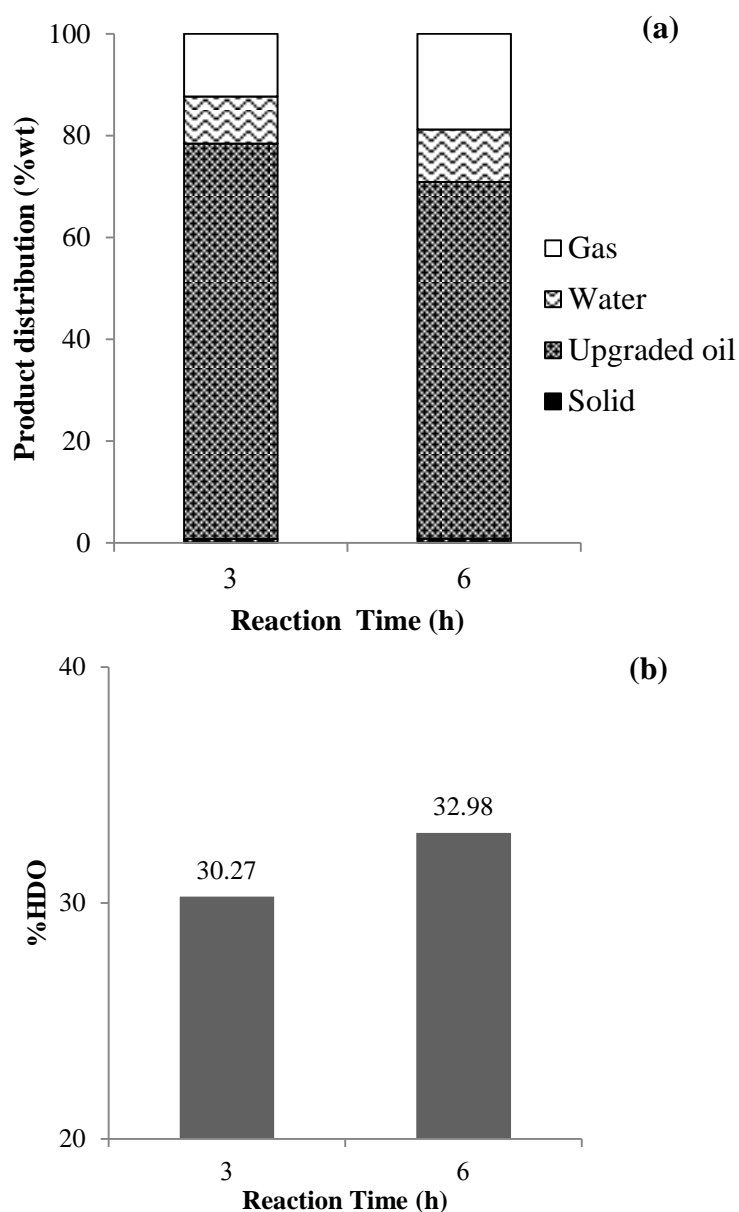
Figure 4.18 The effect of reaction time on catalytic hydrodeoxygenation (a) product distribution and (b) %HDO

With increasing the reaction time, the CO, CO_2, CH_4, C_2H_2, C_2H_4, C_2H_6 and C_3H_8 content increased while the amount of remaining H_2 decreased, as shown in Figure 4.19.
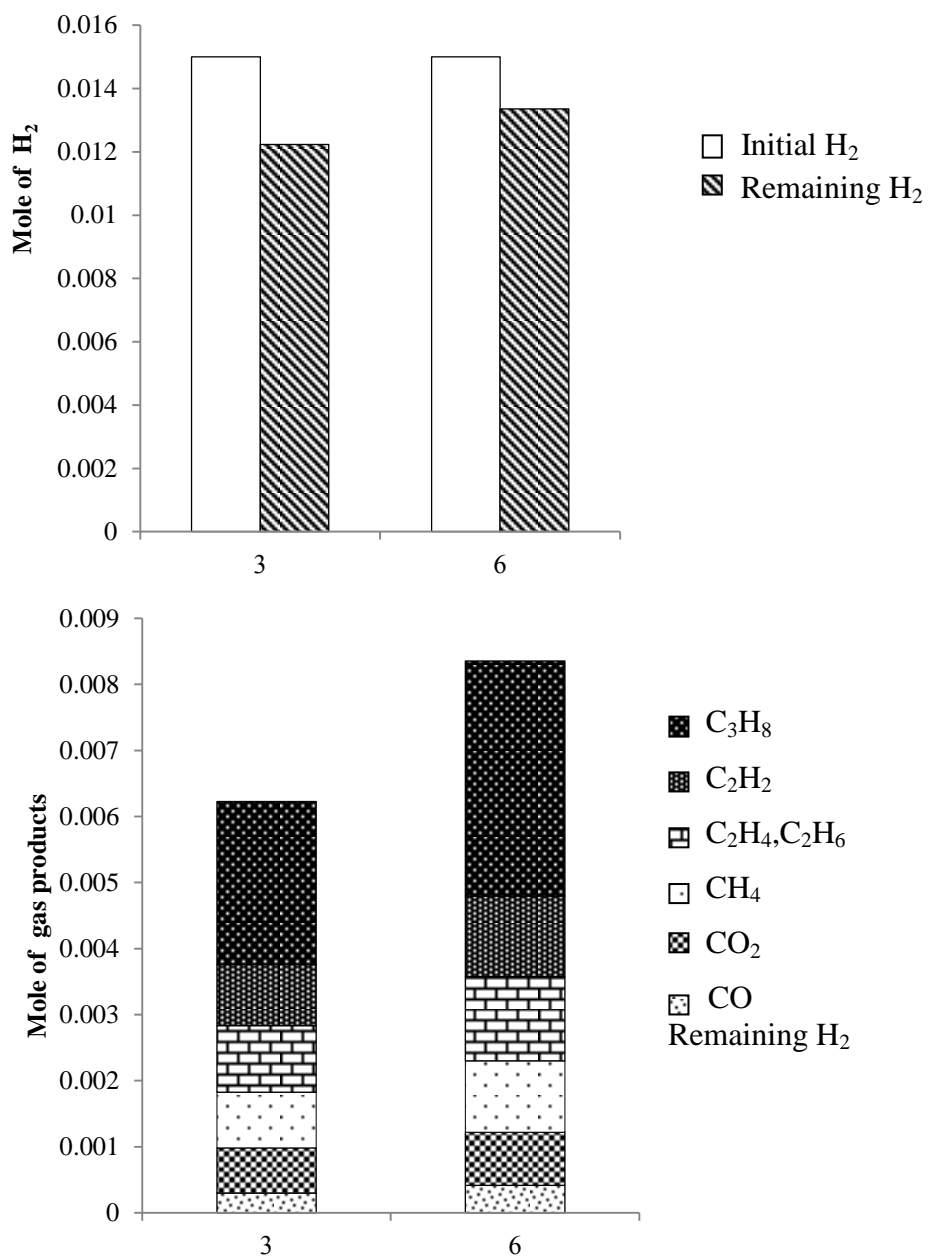
Figure 4.19 The effect of reaction time on catalytic hydrodeoxygenation on the compositions of gas products.

4.4 The Comparison of Bio-Oil Upgrading Activity between Using CoMo/Al$_2$O$_3$ and NiMo/Al$_2$O$_3$

Figure 4.20(a) shows the product distribution from the experiment with the best oxygen removal condition for both catalysts (at 5%wt catalyst, 325°C, 5 bar initial pressure of H$_2$ and 3 hours reaction time). The experiment with CoMo catalyst clearly yielded higher content of solid than NiMo catalyst.
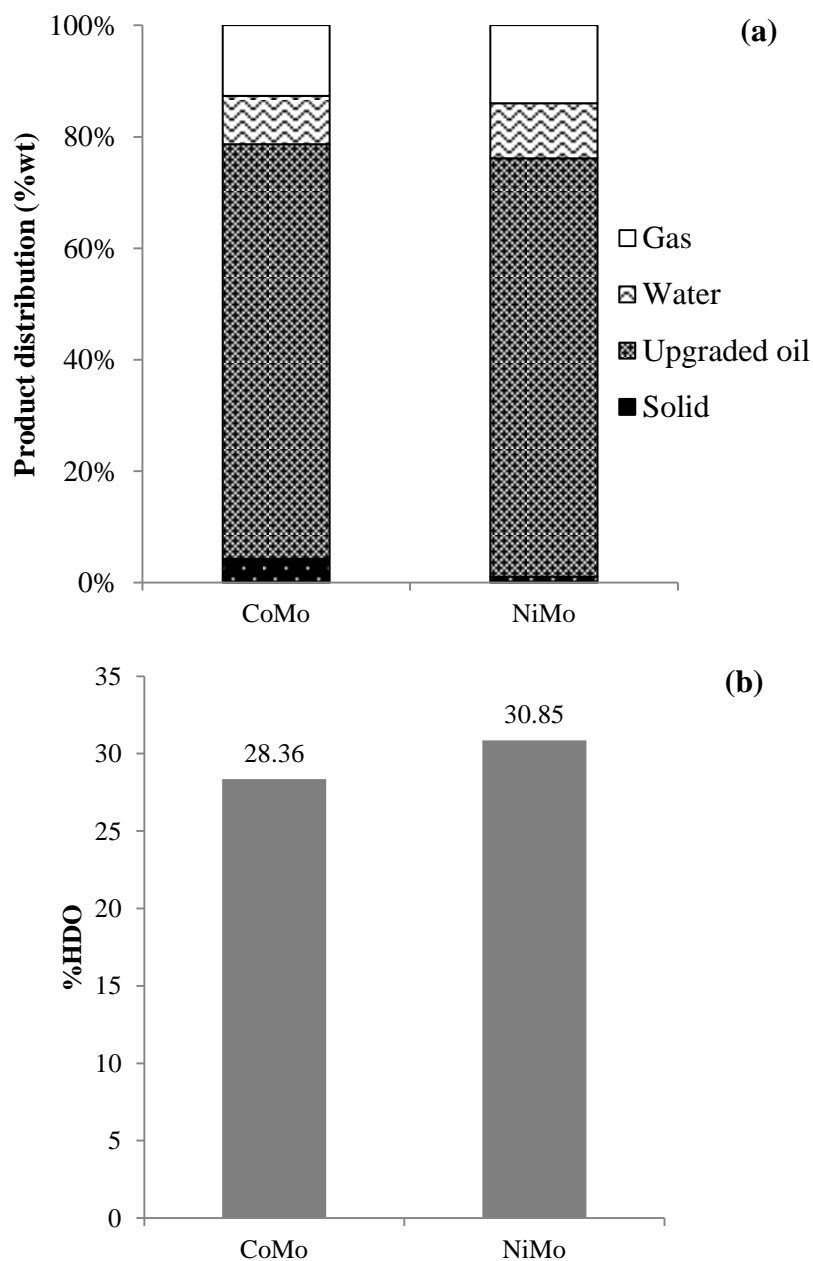
Figure 4.20 The effect of catalyst type on catalytic hydrodeoxygenation (a) product distribution and (b) %HDO

Figure 4.20(b) showed the effect of catalyst type on catalytic hydrodeoxygenation. These results indicated that %HDO of $CoMo/Al_2O_3$ and $NiMo/Al_2O_3$ were 28.36% and 30.85%, respectively. The efficiency of oxygen removal of $NiMo/Al_2O_3$ was higher than that from $CoMo/Al_2O_3$. In addition, the yield of upgraded bio-oil was higher.
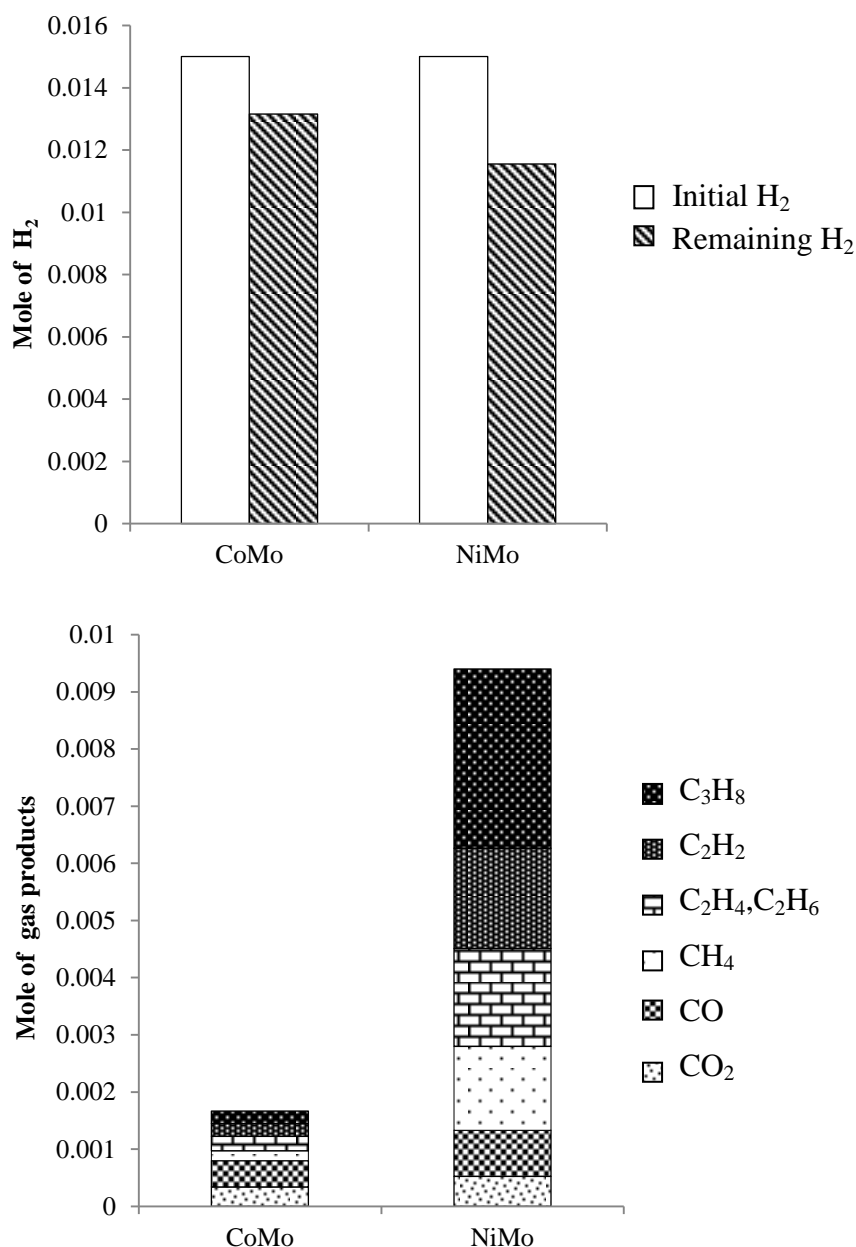
Figure 4.21 The effect of catalyst types on catalytic hydrodeoxygenation on the compositions of gas products.

The gas products of both catalysts had the same composition i.e. CO, CO_2, CH_4, C_2H_2, C_2H_4, C_2H_6 and C_3H_8. However, the $NiMo/Al_2O_3$ clearly showed higher amount of gas product and higher H_2 consumption than $CoMo/Al_2O_3$ as seen in Figure 4.21.

4.5 The Comparison of Upgraded Bio-Oil with conventional liquid Fuels

The poor properties of bio-oil are high oxygen content, corrosive and low heating value when compared with heavy fuel oil. The bio-oil from upgrading experiment which gave the best oxygen removal performance (i.e. using 5% $NiMo/Al_2O_3$ operating at 300 °C, 15 bar of H_2 initial pressure and 3 hours reaction time) was selected for properties comparison with heavy fuel oil. The properties of model bio-oil before upgrading are also given as reference. As seen in Table 4.1, all properties could be improved by catalytic hydrodeoxygenation reaction.

Table 4.1 Comparison of properties of model bio-oil, upgraded bio-oil[1] and heavy fuel oil

Physical property	Model bio-oil	Upgraded Bio-oil[1]	Heavy fuel oil
Moisture content (%wt)	-	11.23	0.1
pH	2.09	3.94	-
Elemental composition (%wt)			
C	62.07	72.94	85
H	6.58	7.43	11
O	31.35	19.63	1.0
N	0	0	0.3
HHV (MJ/kg)	26.15	33.78	40

[1] at 5%wt of $NiMo/Al_2O_3$ catalyst, 300°C, 15 bar of H_2 initial pressure and 3 hours

CHAPTER 5

CONCLUSIONS AND RECOMMENDATIONS FOR FUTURE WORK

5.1 CONCLUSIONS

The problematic property of bio-oil -- The oxygen content -- was improved by the catalytic hydrodeoxygenation (HDO) reaction. The following conclusions are derived from this work:

- To avoid mass transfer limitation, the autoclave reactor was tested with different stirring rates1000 rpm can ensure minimized mass transfer limitation.
- The hydrodeoxygenation in the presence of $CoMo/Al_2O_3$ was able to remove oxygen from the model bio-oil. The efficiency of oxygen removal increased with temperature. However, the high temperatures caused a loss of upgraded bio-oil products by solid formation and oil cracking into gas production as well as the damage on catalyst.
- With the presence of water in bio-oil, the %HDO was considerably reduced due to the deactivation of the catalysts.
- Mass balance showed that the main products of the reaction were in the liquid phase (upgraded bio-oil and water formed by the reaction).
- For the carbon balance, was mostly carbon contained in the liquid product, but the carbon molecules were lost in the form of solid (coke) and gas products.
- Under the conditions studied, the HDO reaction could not be complete due to the insufficient supply of H_2.
- The %HDO increased from 30.27 to 37.38 when the initial pressure of H_2 was increased from 5 to 15 bars.
- Increasing reaction time slightly enhanced the efficiency of the catalyst to remove oxygen from bio-oil.
- The increase in the reaction temperature enhanced the efficiency of the catalyst even more to eliminate the oxygenated molecules in bio-oil for both $NiMo/Al_2O_3$ and $CoMo/Al_2O_3$.
- The NiMo catalyst displayed higher efficiency in oxygen removal than did the CoMo catalyst.

5.2 RECOMMENDATIONS FOR FUTURE WORK

Bio-oils have received extensive recognition from international energy organizations around the world for their characteristics as fuels used in combustors, engines or gas turbines, and resources in chemical industries. Therefore, there are still needs for further studies to improve its properties especially oxygen including in molecule. Recommendations for further studies are described as follows:

- HDO catalyst development should aim at a catalyst sufficiently active for the HDO reaction, but resistant toward water and coke formation.

- As realized from this work, the H_2 initial pressure was limited due to the maximum pressure of the reactor. The semi-continuous or continuous process should be developed and applied to improve the %HDO and then the optimal condition will be tested with real bio-oil. As part of this study, a semi-continuous process was also developed by modifying the existing batch-type process. Initial tests using water and N_2 instead of oil and H_2 were carried out. The details can be referred to in Appendix C

REFERENCES

Adjaye, JD, Bakhshi, NN. (1995), Production of hydrocarbons by catalytic upgrading of a fast pyrolysis bio-oil, Part II: Comparative catalyst performance and reaction pathways, Fuel Process Technology, Vol. 45, pp. 185–202.

Adjaye, JD and Bakhshi, NN. (1995), Production of hydrocarbons by catalytic upgrading of a fast pyrolysis bio-oil, part I: conversion over various catalysts, Fuel Process Technology, Vol. 45, pp. 161–183.

Asphaug, S. (2013),Catalytic Hydrodeoxygenation of Bio-oils with Supported MoP-Catalysts, Engineering Science and Technology,Chemical Engineering, Norwegian University of Science and Technology (NTNU).

Auroux, A. and Gervasini, A. (1991), Acidity and basicity of metal oxide surfaces, J. Catal., 131, pp. 190-198.

Badawi, M. Cristol, S., Paul, J.F., and Payen, E. (2009), DFT study of furan adsorption over stable molybdenum sul de catalyst under HDO conditions, C. R. Chimie 12, pp. 754-761.

Badawi, J. F. Paul, S. Cristol, et al. (2011), Effect of water on the stability of Mo and CoMo hydrodeoxygenation catalysts: A combined experimental and DFT study, Catalysis, Vol. 282, pp. 155-164.

Bakhshi, N.N. and Adjaye, J.D. (1995), Catalytic conversion of a biomass-derived oil to fuels and chemicals I: Model compound studies and reaction pathways, Biomass Bioeng., pp. 131-149.

Beis, S.H., Onay, O and Kockar, O.M. (2002), Fixed-bed pyrolysis of safflower seed: influence of pyrolysis parameters on product yields and compositions, Renewable Energy, Vol. 26, pp. 21-32.

Boucher, M.E., Chaala, A. and Roy C. (2000), Bio-oils obtained by vacuum pyrolysis of softwood bark as a liquid fuel for gas turbines, Part I: Properties of bio-oil and its blends with methanol and a pyrolytic aqueous phase, Biomass Bioenergy, Vol. 19, pp. 337–350.

Bridgwater, A.V. (2002), Fast Pyrolysis of Biomass ,A Handbook,Vol. 2.

Chiaramonti, D., Bonini, M., Fratini, E., et al. (2003), Development of emulsions from biomass pyrolysis liquid and Diesel and their use in engines, Part 1: Emulsion production, Biomass Bioenergy, Vol. 25, pp. 85–99.

Chiaramonti, D., Bonini, M., Fratini, E., et al. (2003), Development of emulsions from biomass pyrolysis liquid and Diesel and their use in engines, Part 2: Tests in Diesel engines, Biomass Bioenergy, Vol. 25, pp. 101–111.

Choi, Y. and Stenger, H.G. (2003), Water gas shift reaction kinetics and reactor modeling for fuel cell grade hydrogen, Journal of Power Sources, Vol. 124, pp. 432-439.

Christensen J. M. Mortensen P. M., Trane R., Jensen P. A., and Jensen A. D. (2009), Effects of H2 and process conditions in the synthesis of mixed alcohols from syngas over alkali promoted cobalt-molybdenum, Appl. Catal. A, Gen. 366, pp. 29-43.

Czernik S, French R, Feik C, et al. (2002), Hydrogen by catalytic steam reforming of liquid byproducts from biomass thermo conversion processes, Industrial & Engineering Chemistry Research, Vol. 41, pp. 4209–4215.

Department of Alternative Energy Development and Efficiency (DEDE) (2011), Potentials and Feasibility Study on Biomass to Liquid Production in Commercial Scale, Executive Summary, pp. 1-32.

Diebold JP. (2005) A review of the chemical and physical mechanisms of the storage stability of fast pyrolysis bio-oil.

Echeandia S, Arias PL, Barrio VL, Pawelec B, Fierro JLG. (2010), Synergy effect in the HDO of phenol over Ni–W catalysts supported on active carbon: Effect of tungsten precursors, Applied Catalysis B: Environmental, Vols. 101(1-2), pp. 1-12.

Fisk A.C., Morgan T., Ji Y., Crocker M.,Crofcheck C. and Lewis S.A. (2009), Bio-oil upgrading over platinum catalysts using in situ generated hydrogen, Applied Catalysis A: General, Vol. 358, pp. 150–156.

Furimsky E. (2000), Catalytic Hydrodeoxygenation, Apply Catalysis A: General, Vol. 199, p. 147.

Furimsky, E. and Massoth F.E. (1999), Deactivation of hydroprocessing catalysts, Catalysis Today, Vol. 52, pp. 381-495. Garcia L, French R, Czernik S, et al. (2000), Catalytic steam reforming of bio-oils for the production of hydrogen: effects of catalyst composition, Apply Catalyst A: General, Vol. 201, pp. 225–239.

Greibrokk T., Lundanes E., Rasmussen K. (2005), Kromatografi, Kromatografi saparasjon og deteksjon, universitetsforlaget,.

Guo XY, Yan YJ and Ren ZW. (2003), The using and forecast of catalyst in biooil upgrading, Acta Energiae Solaris Sinica, Vol. 124, pp. 206–212.

Guo Y, Wang Y, Wei F, et al. (2001), Research progress in biomass flash pyrolysis technology for liquids production, Chemical Industry and Engineering Progress, pp. 13-17.

Gutierreza A., Kailaa R.K. and Krausea A.O.I. (2009), Hydrodeoxygenation of guaiacol on noble metal catalysts, Catalyst Today, Vol. 147, pp. 239-246.

Hogan, E., Robert, J., Grassi, G. and Bridgwater A.V. (1992), Biomass Thermal Processing, Proceedings of the First Canada/European Community R&D Contractors Meeting.

Ikura M, Stanciulescu M, Hogan E. (2003), Emulsification of pyrolysis derived bio-oil in Diesel fuel, Biomass Bioenergy, Vol. 24, pp. 221–232.

Kwon K. C. Mayfeld H., Marolla T., Nichols B., and Mashburn M. (2011), Catalytic deoxygenation of liquid biomass for hydrocarbon fuels, Renew. Energy, 36, pp. 907-915.

Massoth F.E., Politzer P., Concha M.C. (2006), Catalytic hydrodeoxygenation of methyl-substituted phenols: Correlations of kinetic parameters with molecular properties, Physical Chemistry B, Vol. 110, pp. 14283-14291.

Moberg D. R. Thibodeau T. J., Amar F. G., and Frederick B. G. (2010), Mechanism of hydrodeoxygenation of acrolein on a cluster model of MoO3, J. Phys. Chem.C, 114, pp. 13782-13795.

Mortensen P.M. (2013), Catalytic Conversion of Bio-oil to Fuel for Transportation. Ph.D. Thesis report, Chemical and Biochemical Engineering, Technical University of Denmark.

Nokkosmaki MI, Kuoppala ET, Leppamaki EA, et al. (2000), Catalytic conversion of biomass pyrolysis vapours with zinc oxide, Journal of Analytical and Applied Pyrolysis, Vol. 55, pp. 119–131.

Oasmaa A, Czernik S. (1999), Fuel oil quality of biomass pyrolysis oils-state of the art for the end-users, Energy Fuels , Vol. 13, pp. 914–921.

Oasmaa A. Kuoppala E., Ardiyanti A. R., Venderbosch R. H., and Heeres H. (2010), Characterization of hydrotreated fast pyrolysis liquids, Energy Fuels 24, pp. 5264-5272.

Ozcimen D, Karaosmanoglu F. (2004), Production and characterization of bio-oil and biochar from rapeseed cake, Renewable Energy, Vol. 29, pp. 779–787.

Payormhorm J.,Kangvansaichol K. , Reubroycharoen P.,Kuchonthara P., Hinchiranan N. (2011), Upgrading of bio-oil derived from pyrolysis of biomass via deoxygenation catalyzed by Pt/Al2O3. Peng WM and Wu QY (2000), Production of fuels from biomass by pyrolysis, New Energy Source, pp. 39-44.

Prins R. (2008), Handbook of Heterogeneous Catalysis, chapter 13.2: Hydrotreating, John Wiley & Sons, Inc., New York.

Ravindranath B. (1989), Principles and practice of chromatography, Ellis Horwood Limited.

Romero Y. Richard F., and Brunet S. (2010), Hydrodeoxygenation of 2-ethylphenol as a model compound of bio-crude over sul ded Mo-based catalysts: promoting effect and reaction mechanism, Appl. Catal. B, Environ. 98, pp. 213-223.

Ryymin E. M. Honkela M. L., Viljava T.R., and Krause A. O. (2010), Competitive reactions and mechanisms in the simultaneous HDO of phenol and methyl heptanoate over sulphided NiMo/γ -Al2O3, Appl. Catal. A: Gen., 389, pp. 114-121.

Ryymin E.M. Honkela M. L. , Viljava T.R., and Krause A. O. I.. (2009), Insight to sulfur species in the hydrodeoxygenation of aliphatic esters over sulphided NiMo/γ -Al2O3, Appl. Catal. A: Gen., 358, pp. 42-48.

Samolada M. C, Baldauf W.and Vasalos I. (1998), A Production of a Bio-Gasoline by Ugrading Biomass Flash Pyrolysis Liquids via Hydrogen Processing and Catalytic Cracking, Fuel, Vol. 77, p. 1667.

Scahill J, Diebold JP, Feik C. (1996), Removal of residual char fines from pyrolysis vapors by hot gasification, Developments in thermochemical biomass conversion, Blackie Academic and Professional, London.

Scholze B and Meier D. (2001), Characterization of the water-insoluble fraction from pyrolysis oil (pyrolytic lignin) Part I. PY-GC/MS, FTIR, and functional groups, Journal of Analytical and Applied Pyrolysis, Vol. 60, pp. 41–54.

Senol O.I. (2007), Hydrodeoxygenation of aliphatic and aromatic oxygenates on sulphided catalysts for production of second generation biofuels, Dissertation for the degree of Doctor of Science in Technology, Helsinki University of Technology, Espoo, Finland.

Senol O. I. Ryymin E.M., Viljava T.R., and Krause A. O. I. (2007), Effect of hydrogen sulphide on the hydrodeoxygenation of aromatic and aliphatic oxygenates on sulphided catalysts, J. Mol. Cat. A: Chem. 277, pp. 107-112.

Senol O. I. Viljava T.R. , and Krause A. O. I. (2007), Effect of sulphiding agents on hydrodeoxygenation of aliphatic esters on sulphided catalysts, Apply Catalysis. A: General 326, pp. 236-244.

Senol O.I., Viljava T.R., Krause AOI. (2005), Hydrodeoxygenation of methyl esters on sulphidedNiMo/c-Al2O3 and CoMo/c-Al2O3 catalysts, Catalyst Today, Vol. 100, pp. 331-335.

Shabaker J.W., and Dumesic J.A. (2004), Kinetics of aqueous-phase reforming of oxygenated hydrocarbons: Pt/Al2O3 and Sn-modified Ni catalysts, Industrial and Engineering Chemistry Research, Vol. 43, pp. 3105-3112.

Sipilae` K, Kuoppala E, Fagernae`s L, et al. (1998), Characterization of biomass–based flash pyrolysis oils, Biomass Bioenergy, Vol. 14(2), pp. 103–113.

Takanabe K Aika K, Seshan K, et al. (2004), Sustainable hydrogen from bio-oil–steam reforming of acetic acid as a model oxygenate, Journal of Catalyst, Vol. 227, pp. 101–108.

Toba M., Abe Y., Kuramochi H., Osako M. and Yoshimura Y. (2011), Hydrodeoxygenation of waste vegetable oil over sulfide catalysts, Catalysis Today 164, pp. 533-537.

Topsoe, H., Clausen, B.S., Massoth, F.E. (1996), Hydrotreating Catalysis Science and Technology Anderson J.R.&Boudart M., Springer, Berlin.

The Japan Institute of Energy (2008), A Guide for Biomass Production and Utilization, The Asian Biomass Handbook.

Venderbosch RH , Ardiyanti AR , Wildschut J , Oasmaa A and Heeres HJ (2010), Stabilization of biomass-derived pyrolysis oils, Journal of Chemical Technology & Biotechnology 85, Vol. 5, pp. 674-686.

Wang D, Czermik S and Chornet E. (1988), Production of hydrogen from biomass by catalytic steam reforming of fast pyrolytic oils, Energy Fuels, Vol. 12, pp. 19–24.

Wang D, Czernik S, Montane´ D, et al. (1997), Biomass to hydrogen via pyrolysis and catalytic steam reforming of the pyrolysis oil and its fractions, Industrial & Engineering Chemistry Research, Vol. 36, pp. 1507–1518. Whiffen J. and Smith K. (2010), Hydrodeoxygenation of 4-methylphenol over unsupported MoP, MoS2 , and MoOx catalysts, Energy Fuels, 24, pp. 4728-4737.

Wildschut J., Mahfud F. H., Venderbosch R. H., and Heeres H. J (2009), Hydrotreatment of fast pyrolysis oil using heterogeneous noble-metal catalysts, Ind. Eng.Chem. Res. 48, pp. 10324-10334.

Yuenyongchaiwat P (2010), Bio-oil Production from Various Biomass Feedstocks by Vacuum Pyrolysis, Thesis Submitted Report, JGSEE.

APPENDIX

This appendix has 3 sections: the first section presents the calculation of bio-oil upgrading results, the second section contains the analysis data of products, and the third section shows the development of a semi-continuous process.

APPENDIX A: CALCULATION OF RESULTS

Example: The Calculation of the %Yield Product from Catalytic Hydrodeoxygenation

The upgrading condition of catalytic hydrodeoxygenation of model bio-oil without water using 5 %wt $CoMo/Al_2O_3$ operated at 325 °C for 3 hours.

The bio-oil weight input in reactor (W_o) is 25 g. After reaction, the weight of liquid product (W_{aq}), which was collected from the reactor was 20.76 g. The % yield of moisture in the liquid product is:

$$\%W_{aq} = \frac{W_{aq}}{W_o} \times 100 = \frac{20.76\ g}{25\ g} \times 100 = 83.05\%.$$

The moisture in the liquid product ($\%H_2O$) is 10.49 %. The %yield of moisture in the liquid product ($\%W_m$) was:

$$\%W_m = \frac{\%H_2O}{100} \times \%W_{aq} = \frac{10.49}{100} \times 83.05 = 9.90\ \%.$$

The upgraded oil in the liquid product ($\%W_u$) was:

$$\%W_u = \%W_{aq} - \%W_m = 83.05 - 9.90 = 75.1\%.$$

The weight of solid product (W_s) is 2.33 g and the catalyst weight input in the reactor W_c is 1.25 g. The % yield of the solid product was:

$$\%W_s = \frac{W_s - W_c}{W_o} \times 100 = \frac{2.33\ g - 1.25 g}{25\ g} \times 100 = 4.30\ \%$$

Thus, the gas product W_g was:

$$\%W_g = 100 - \%W_{aq} - \%W_s = 100 - 83.05 - 4.30 = 8.63$$

Example : The Calculation of the Mole of the Gas Product

The upgrading condition of the catalytic hydrodeoxygenation of the model bio-oil without water using 5 %wt $CoMo/Al_2O_3$ was operated at 325 °C for 3 hours. The volume of gas product which was measured by using gas syringe was 4300 mL.

Standard calibration curve

The peak area of 1% by volume of CO_2 gas with 2 mL sampling volume was 30459.9, and then the standard calibration curve between concentration and peak area was plotted as shown below.
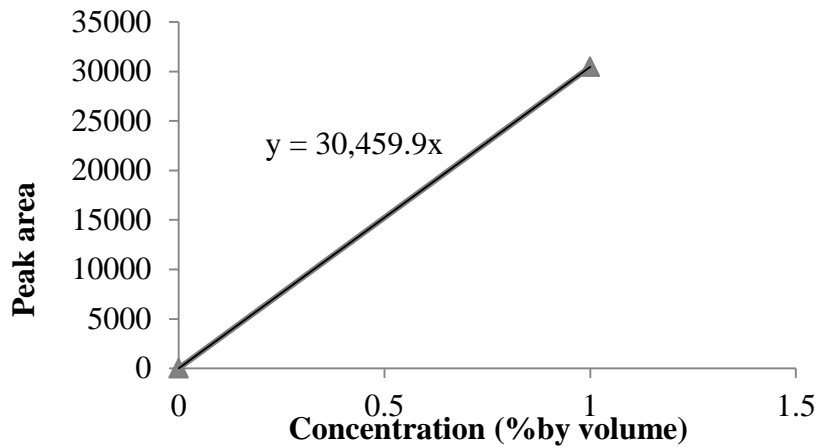
Figure A1. Standard calibration curve of CO_2

The peak area of CO_2 in the gas product with 2 mL sampling volume was 20521.8.
The % concentration of CO_2 was:

$$\% \text{ Conc. of } CO_2 \text{ gas} = \frac{20521.8}{30459.9} = 0.67\% \text{ by volume}$$

$$Conc. of\ CO_2\ in\ gas\ product = \frac{0.67\ ml\ _{CO_2}}{100\ ml_{total}} \times \frac{1\ mol_{CO_2}}{22.4\ l_{CO_2}} \times \frac{1\ l_{CO_2}}{1000\ ml_{CO_2}} = 0.0000003\ \frac{mol_{CO_2}}{ml_{total}}$$

The total volume of the gas product was 1520 ml. So, the mole of CO_2 in the gas product was:

$$Mole\ of\ CO_2\ in\ gas\ product = 0.0000003\ \frac{mol_{CO_2}}{ml_{total}} \times 1520\ ml_{total} = 0.00046\ mol_{CO_2}$$

APPENDIX B: RAW DATA

Table B.1 The product distribution of catalytic hydrodeoxygenation using $CoMo/Al_2O_3$

Water (in bio-oil) (%wt)	Catalyst %(w/w)	Temperature (°C)	Initial pressure of H_2 (bar)	Stirring velocity (rpm)	Reaction Time (hour)	Weight (g)		Water (in upgraded bio-oil) (%wt)
						Liquid	Solid	
-	1	250	3	1000	3	22.01	0.00	7.6
-	1	300	3	1000	3	18.00	0.00	8
-	1	325	3	1000	3	12.08	6.90	8.14
-	1	350	3	1000	3	9.24	7.63	10.63
20	1	325	3	1000	3	12.95	5.68	26.27
-	1	300	3	500	3	14.49	6.36	9.7
-	1	300	3	750	3	18.79	0.00	9.71
-	1	300	3	1000	3	20.74	0.00	9.75
-	1	325	5	750	3	21.01	2.16	9.71
-	5	325	5	750	3	20.76	1.08	10.49

Table B. 2 The product distribution of catalytic hydrodeoxygenation using NiMo/Al$_2$O$_3$

Catalyst %(w/w)	Temperature (°C)	Initial pressure of H$_2$ (bar)	Stirring velocity (rpm)	Reaction Time (hour)	Weight (g)		Water (in upgraded bio-oil) (%wt)
					Liquid	Solid	
5	275	5	750	3	21.81	1.30	9.65
5	300	5	750	3	21.71	0.20	10.59
5	325	5	750	3	21.25	0.26	11.65
5	300	5	750	3	21.72	0.20	10.59
5	300	10	750	3	21.29	0.02	11.53
5	300	15	750	3	21.46	0.13	11.23
5	300	5	750	6	20.09	0.22	12.87

Table B.3 The chemical analysis of catalytic hydrodeoxygenation using $CoMo/Al_2O_3$

Water (%wt)	CoMo catalyst (%wt)	Temperature (°C)	H_2 initial pressure (bar)	Stirring velocity (rpm)	Reaction Time (hour)	Elemental Analysis			%HDO
						C	H	O	
-	1[1]	300	3	1000	3	68.82	7.46	23.72	8.97
-	1[1]	250	3	1000	3	68.13	6.98	24.89	3.33
-	1[1]	300	3	1000	3	68.82	7.46	23.72	8.97
20	1[1]	325	3	1000	3	69.79	7.75	22.46	13.51
-	1[1]	350	3	1000	3	60.31	6.95	32.74	1.81
-	1[2]	325	5	750	3	64.83	8.49	26.68	16.60
-	5[2]	325	5	750	3	66.74	8.33	24.94	22.05

[1]$CoMo/Al_2O_3$ size 1- 3 mm

[2]$CoMo/Al_2O_3$ size 0.5-1.0 mm

Table B.4 The chemical analysis of catalytic hydrodeoxygenation using NiMo/Al$_2$O$_3$[1]

Catalyst %(w/w)	Temperature (°C)	H$_2$ initial pressure (bar)	Stirring velocity (rpm)	Reaction Time (hour)	Elemental Analysis			%HDO
					C	H	O	
5	275	5	750	3	69.90	6.91	23.19	26.03
5	300	5	750	3	70.71	7.43	21.86	30.27
5	300[2]	5	750	3	70.88	7.37	21.75	30.62
5	325	5	750	3	70.58	7.74	21.68	30.85
5	300	10	750	3	70.86	7.74	21.40	31.74
5	300	15	750	3	72.94	7.43	19.63	37.38
5	300	5	750	6	71.82	7.17	21.01	32.98

[1]NiMo/Al$_2$O$_3$ size 0.5-1.0 mm

[2]Experimental repeatability

Table B.5 The compositions of gas products

Catalyst	%wt water	Temperature (°C)	H₂ initial pressure (bar)	Reaction time (h)	Mole of gases product						
					H_2	CO	CO_2	CH_4	C_2H_4, C_2H_6	C_2H_2	C_3H_8
CoMo	-	250	1	3	0.0079	0.00015	0.00052	0.00004	0.00003	0.00002	0.00002
	-	300	1	3	0.0068	0.00034	0.00052	0.00012	0.00011	0.00009	0.00008
	-	325	1	3	0.0067	0.00049	0.00065	0.00025	0.00039	0.00040	0.00030
	-	350	1	3	0.0082	0.00173	0.00132	0.00125	0.00106	0.00079	0.00057
	-	325	1	3	0.0081	0.00064	0.00030	0.00011	0.00014	0.00011	0.00011
	-	325	5	3	0.0132	0.00034	0.00046	0.00017	0.00025	0.00022	0.00022
	20	325	1	3	0.0074	0.00031	0.00071	0.00010	0.00011	0.00006	0.00004
NiMo	-	275	5	3	0.0124	0.00025	0.00058	0.00042	0.00042	0.00037	0.00167
	-	300	5	3	0.0122	0.00039	0.00069	0.00082	0.00097	0.00093	0.00256
	-	325	5	3	0.0118	0.00052	0.00081	0.00147	0.00172	0.00175	0.00314
	-	300	10	3	0.0226	0.00035	0.00071	0.00086	0.00093	0.00086	0.00261
	-	300	15	3	0.0422	0.00062	0.00033	0.00080	0.00093	0.00073	0.00333
	-	300	5	6	0.0134	0.00042	0.00081	0.00108	0.00127	0.00122	0.00356

Table B6 GC-MS analysis of catalytic hydrodeoxygenation using CoMo/Al$_2$O$_3$

Chemical name	Retention time (min)	%Area								
		No cat	Stirring velocity			No water bio-oil				20% water bio-oil
			500rpm	750rpm	1000rpm	250 °C	300 °C	325 °C	350 °C	325 °C
Acetaldehyde	0.13	-	-	-	-	-	-	-	-	0.13
Ethanol	1.4	4.9	4.84	4.32	4.56	5.54	4.56	3.32	2.01	5.38
Acetone	1.44	12.931	12.55	12.3	12.6	12.47	12.6	9.48	6.86	11.11
2-Methylfuran	1.73	-	-	-	-	-	-	0.41	-	0.47
Ethyl acetate	1.76	9.876	9.6	9.52	9.76	10.01	9.76	7.86	4.15	6.79
Acetic acid	1.88	-	-	-	-	-	-	-	1.65	1.12
4-Methyl-2-pentanone	2.94	-	-	-	-	-	-	0.36	-	-
1,2,4-Trimethylbenzene	7.41	-	-	-	-	-	-	0.13	0.11	-
phenol	8.29-8.39	62.58	60.44	62.06	62.17	62.85	62.17	55.77	51.07	63.87
Phenylpropyl ether	9.16	-	-	-	-	-	-	0.09	-	-
Benzyl alcohol	9.69	-	0.03	0.02	0.01		0.01	-	-	-
phenyl acetate	10.15	0.419	0.29	0.35	0.32	0.29	0.32	-	-	-
2-methyl phenol	10.25-10.36	-	0.55	-	-		-	-	-	0.77
1-(2-Furyl)-butan-3-one	10.52	0.945	-	0.3	0.25	0.55	0.25	-	-	0.17
4-Methylphenol	10.91-10.98	-	-	-	-	-	-	0.08	0.59	0.06
2-methylbenzofuran	11.43	0.52	0.62	0.59	0.54	-	0.54	1.03	0.91	0.58
2-ethyl phenol	12.56	-	-	0.68	0.29	-	0.29	4.38	4.34	0.76
4-ethylphenol	13.25	-	-	-	-	-	-	1.51	1.04	-
2-(1-methylethyl)-phenol	14.07	0.161	0.85	0.64	0.44	-	0.44	1.39	1.29	-
2,3-Dimethylbenzofuran	14.32	0.154	0.77	0.41	0.3	-	0.3	0.89	0.72	0.36
3-(1-Methylethyl)phenol	14.58	-	-	-	-	-	-	0.69	0.38	0.38
1,2,3,4-Tetrahydro-6,7- dimethylnapthalene	15.77	-	-	-	-	-	-	0.51	0.43	-
Diethylphenol	16.13	-	-	-	-	-	-	0.17	-	-
3-Methylcarbazole	20.68	-	-	-	-	-	-	0.36	0.35	-
9H-Xanthene	20.81	0.264	0.22	0.2	0.15	-	0.15	0.51	0.46	0.33
4H-Pyrido[1,2-a]pyrimidine-3-caxylic acid,1,6,7,8,9,9a-hexahydro-4-oxo-,ethyl ester	23.29	0.297	0.21	0.22	-	-	-	0.29	0.12	0.2
1,4-Dimethoxyphenanthrene	23.79	0.151	0.08	-	-	-	-	0.11	-	-
(7E,9Z)-7,9-Dodecadien-1-ly acetate	25.57	-	-	-	-	-	-	0.24	-	0.18
Total	97.92	95.16	95.67	94.45	96.24	94.45	89.94	76.5	92.53	94.1

APPENDIX C: THE DEVELOPMENT OF A SEMI-CONTINUOUS PROCESS

A semi-continuous process (see Figure C.1), which allows a continuous supply of H_2, was modified from the existing batch-type process to improve the %HDO by allowing H_2 supply, while keeping the operating pressure below the maximum pressure designed for the reactor. H_2 was continuously supplied through an inlet valve at a regulated pressure. The pressure inside the reactor was controlled by a solenoid valve installed at the gas outlet line. The value would automatically release the gas product out when the pressure exceeded the predetermined value or add more H_2 to the reactor to maintain the pressure. In the initial experiments, the water and N_2 were used instead of bio-oil and H_2, respectively.

Figure C.1 The high pressure autoclave reactor (semi-continuous proces)